

HETEROGENEOUS MULTISCALE FEM FOR DIFFUSION PROBLEMS ON ROUGH SURFACES*

ASSYR ABDULLE[†] AND CHRISTOPH SCHWAB[‡]

Abstract. We present a finite element method for the numerical solution of diffusion problems on rough surfaces. The problem is transformed to an elliptic homogenization problem in a two dimensional parameter domain with a rapidly oscillating diffusion tensor and source term. The finite element method is based on the heterogeneous multiscale methods of E and Engquist [*Commun. Math. Sci.*, 1 (2003), pp. 87–132]. For periodic surface roughness of scale ε and amplitude $O(\varepsilon)$, the method converges at a robust rate, i.e., independent of ε , to the homogenized solution.

Key words. rough surfaces, multiscale finite element method, diffusion problems

AMS subject classification. 65N30

DOI. 10.1137/030600771

1. Introduction. Diffusion on rough surfaces is a basic problem for many applications. Without attempting to be exhaustive, we mention the following: in biology, for the transport of molecules in living cells as, for example, the transport of lipids on the cell membrane, where compartmentalization of the membrane confines the diffusion [14]; in porous media flow, where the fracture of rock and pore volumes induce local geometry which has to be taken into account for the flow transport [2], [19]; in material science, where rough surfaces arise in the study of diffusion in crystals with topological defects [4]. Finally, they also arise in the study of thermal or electrical conduction in fractures [22].

Accurate numerical solution of diffusion problems is by now standard, unless the problem contains multiple length scales. Then small physical length scales in the problem must either be resolved by the discretization or be accounted for by some form of upscaling or homogenization prior to the numerical solution of the problem. When the data of the problem is oscillatory with a small period, classical two-scale approaches are well established, and the analytical treatments lead to homogenized equations (see, e.g., [5], [9]) with regular, i.e., slowly varying, coefficients.

The fine scale behavior, i.e., the oscillations of the solution, are lost in the homogenization process but can be recovered through the solution of additional “corrector” problems after the solution of the homogenized equation. These corrector problems, however, again exhibit rapidly oscillating coefficients so that their accurate numerical solution is as expensive as that of the original problem.

Numerical methods for homogenization problems have been considered by several authors. They were first studied by Babuska [3] for elliptic problems in one dimension, for which he proposed a finite element method (FEM) on a macroscale grid with basis functions which capture the solution’s microscopic behavior, and by Engquist [13]

*Received by the editors August 29, 2003; accepted for publication (in revised form) April 19, 2004; published electronically January 24, 2005.

<http://www.siam.org/journals/mms/3-1/60077.html>

[†]Department of Mathematics, University of Basel, Rheinsprung 21, CH-4051 Switzerland (assyrd.abdulle@unibas.ch). This author’s work was partially supported by the Swiss National Foundation under grant 200021-103863/1 and was partially done during his stay at CoLab, ETH Zürich.

[‡]Seminar for Applied Mathematics, ETH Zürich, CH-8092 Switzerland (schwab@math.ethz.ch). This author’s work was performed in the network “HMS 2000” HPRN-CT-2000-00109 and was supported by the Swiss BBW under grant BBW 01.0025-1, and the Swiss National Foundation under grant 21-58754.99.

for dynamic problems. Hou and Wu [16] and Hou, Wu, and Cai [17] extended these ideas to more than one dimension and possibly nonperiodic fine scale behavior of the coefficients. In these “adapted shape function” approaches, however, in each macroelement solution adapted microshape functions have to be precomputed by a standard FEM resolving the fine scale of the problem, and its complexity depends on the small length scale to be resolved. Error analysis is available in [3], [16], [17] for periodic coefficients.

In [20], [24] a two-scale FEM based again on adapted trial and test functions was introduced, and its exponential convergence rate, independently of the scale parameter ε , was established even in the absence of high regularity of the solution on the fine scale. In this analysis, it was assumed that the coefficients are periodic in the fine scale and that the cell problem can be solved exactly.

Heterogeneous multiscale methods (HMM) have been introduced in [11] as a general framework for the numerical computation of solutions to problems with multiple scales. Its main objective is to avoid the precomputation of fine scale shape functions as well as of the coefficients of the homogenized equation. In a FE context for elliptic problems, this method discretizes the physical problem directly by a “macroscopic FEM” model which does not (and cannot) resolve the fine scales of the solution. Derivation of “homogenized” equations is not necessary, and the correct microscale behavior can be reconstructed with additional solves from the known macroscopic solution. The fine scale of the problem is accounted for in the elements’ stiffness matrix calculations, where, in place of numerical integration, the fine scale problem is accessed either by solving a unit-cell problem or by solving a problem on a patch with a fixed, i.e., scale-independent, number of unit cells. This is also the case when homogenized coefficients are precomputed, the present approach, however, has advantages: while in [12] the analysis of the method relies on periodic models of the fine scale, the algorithm itself does not (although the error analysis of the algorithm in the nonperiodic case is open).

A finite difference method based on this strategy has been proposed in [1] for parabolic multiscale problems. Its analysis is done for the periodic case, but the method applies to more general problems with time dependent, rough correlated (random) coefficients. It is also applicable to nonconservative problems. An error analysis of the hierarchic multiscale method for periodic elliptic homogenization problems has been given in [12], where stationary ergodic random coefficients and nonlinear problems are also addressed and analyzed in some cases.

In diffusion problems on rough surfaces considered here, the small length scales enter through fine structures of the surface. In some situations (as, for example, for crystalline objects, cell membranes, etc.), these fine structures can be obtained to high resolution (beyond that of typical FE calculations) by modern scanning and microscopy techniques (see, e.g., [10]). In order to compute macroscopic information on the solution (such as mean diffusion rates on the surface), full resolution of the fine scale in the data is not necessary, as we show below, provided the fine scale is “uniform” throughout the physical domain.

We apply here the FEM of “heterogeneous multiscale” type of [11], [12] for the numerical solution of stationary diffusion problems on such rough surfaces Γ^ε . While for a standard FEM one needs to triangulate the whole surface with a mesh which resolves the oscillation of the surface, the present method resolves the surface’s fine scale only on small sampling domains within a macrotriangulation of the underlying smooth surface. The surface roughness of Γ^ε is modeled by assuming a rapidly oscillating, *periodic* perturbation with length scale and amplitude ε about a mean

surface Γ^0 which we assume for our analysis to be smoothly curved (the algorithm is also applicable to polyhedral “mean” surfaces, but an analysis in this setting is yet to be done). Under the above assumptions, the diffusion problem on an oscillating surface can be transformed into a well-posed elliptic problem on a flat domain with an oscillatory diffusion tensor. We show then how to further transform this problem with an oscillatory right-hand side into a standard elliptic homogenization problem, apply the heterogeneous multiscale FEM (HM FEM) to it, and give error estimates for the numerical solution. Although the numerical method proposed is similar to [11], [12], there are also differences: in the solution of the microproblems, we do not impose periodic boundary conditions strongly on the FE space but rather enforce these only weakly through Lagrange multipliers. This, in turn, allows more flexibility in meshing the unit cell, as required, e.g., in adaptive mesh refinement. Likewise, the macroscopic data enters the microcalculation only through Lagrange multipliers; in this way, the scales are only weakly coupled or “mortared” while the error estimates of [12] still hold. We emphasize that the assumption of periodicity of the oscillations is essential in the error estimates—while the algorithm is applicable also in the non-periodic setting, *no derivation of error bounds for deterministic, nonperiodic rough coefficients is known to us*.

We consider the following elliptic problem:

$$(1.1) \quad -\nabla_{\Gamma^\varepsilon} \cdot (D^{\tilde{\varepsilon}} \nabla_{\Gamma^\varepsilon} u) = f \text{ in } \Gamma^\varepsilon, \quad u = 0 \text{ on } \partial\Gamma^\varepsilon,$$

where $\nabla_{\Gamma^\varepsilon}$ is the tangential gradient on Γ^ε , an oscillatory surface with surface oscillations occurring at length scale ε . The diffusion tensor $D^{\tilde{\varepsilon}}$ is given in a basis of the tangent space $T_x\Gamma^\varepsilon$ at a point x of the surface. We also assume that $D^{\tilde{\varepsilon}}(x) = D(x, \frac{x}{\tilde{\varepsilon}}) = D(x, y)$ is symmetric and 1-periodic w.r.t. $y_1, y_2 \forall x \in \Gamma^\varepsilon$, that $D_{ij}(x, \cdot) \in L^\infty(\mathbb{R}^2)$, and that $x \rightarrow D_{ij}(x, \cdot)$ is smooth from $\bar{\Gamma}^\varepsilon \rightarrow L^\infty(\mathbb{R}^2)$. Furthermore, we assume that $D^{\tilde{\varepsilon}}(x)$ is uniformly elliptic.

REMARK 1.1. *The length scale ε of the surface’s oscillation can be different from the oscillation $\tilde{\varepsilon}$ in the diffusion tensor $D^{\tilde{\varepsilon}}$, provided $\varepsilon = n_1\tilde{\varepsilon}$ or $\tilde{\varepsilon} = n_2\varepsilon$, where $n_1, n_2 \in \mathbb{N}$.*

To expose the heterogeneous multiscale FEM, we further restrict ourselves to the model problem

$$(1.2) \quad -\Delta_{\Gamma^\varepsilon} u^\varepsilon = f \text{ in } \Gamma^\varepsilon, \quad u^\varepsilon = 0 \text{ on } \partial\Gamma^\varepsilon,$$

where $\Delta_{\Gamma^\varepsilon} = \nabla_{\Gamma^\varepsilon} \cdot \nabla_{\Gamma^\varepsilon}$ is the Laplace–Beltrami operator (the general case is obtained by changing the metric but does not introduce any new technical difficulties into our method or our analysis). Throughout, we add a superscript on the solution u to emphasize its dependence on ε .

The paper is organized as follows. In section 2 we define the family of surfaces considered. In section 3 we describe how (1.2) (or (1.1)) can be transformed into a homogenized problem on the reference domain of the parameterized surface. In section 4 we describe the multiscale numerical method used and give error estimates. Finally, in section 5, we give numerical examples to illustrate the performance of our method.

2. Setting of the problem. In this section we define the family of surfaces we will consider.

Notation. In what follows, c and c_i denote generic constants whose value can change at any occurrence but depend only on the quantities which are indicated explicitly. We will use the notation $g^{-T} := (g^{-1})^T$. To simplify notation we will also denote

the partial derivatives $\partial/\partial z_i$ by ∂_i if no confusion occurs. For $r = (r_1, r_2) \in \mathbb{N} \times \mathbb{N}$, we denote $|r| = r_1 + r_2$, $D^r = \partial_1^{r_1} \partial_2^{r_2}$. We will consider the usual Sobolev space $H^1(\Omega) = \{u \in L^2(\Omega); D^r u \in L^2(\Omega), |r| \leq 1\}$ with norm $\|u\|_{H^1(\Omega)} = (\sum_{|r| \leq 1} \|D^r u\|_{L^2(\Omega)}^2)^{1/2}$. We will also consider $H_0^1(\Omega)$ the closure of $C_0^\infty(\Omega)$ for the $\|\cdot\|_{H^1(\Omega)}$ norm and the spaces $W^{1,p}(\Omega) = \{u \in L^p(\Omega); D^r u \in L^p(\Omega), |r| \leq 1\}$ and $W^{2,\infty}(\Omega) = \{u \in L^\infty(\Omega); D^r u \in L^\infty(\Omega), |r| \leq 2\}$.

2.1. The family of surfaces. Let Ω be a bounded subset of \mathbb{R}^2 . We consider a family of surfaces $\Gamma^\varepsilon \subset \mathbb{R}^3$ parameterized by

$$(2.1) \quad \begin{aligned} F^\varepsilon : \bar{\Omega} &\longrightarrow \mathbb{R}^3, \\ (\xi_1, \xi_2) &\longrightarrow F^0(\xi) + \varepsilon a^\varepsilon(\xi) n^0(\xi), \end{aligned}$$

where $\xi = (\xi_1, \xi_2) \in \bar{\Omega}$, $F^\varepsilon(\Omega) = \Gamma^\varepsilon$, $F^0(\Omega)$ parameterize a smooth surface $\Gamma^0 \subset \mathbb{R}^3$, a^ε is a rough coefficient (see below), and

$$(2.2) \quad n^0(\xi) = \frac{\partial_1 F^0(\xi) \times \partial_2 F^0(\xi)}{\|\partial_1 F^0(\xi) \times \partial_2 F^0(\xi)\|_2}.$$

We also define the coefficients of the first fundamental form of $\Gamma^\varepsilon, \Gamma^0$ (see subsection 2.2) by

$$(2.3) \quad g_{ij}^\varepsilon = \langle \partial_i F^\varepsilon, \partial_j F^\varepsilon \rangle \quad \text{and} \quad g_{ij}^0 = \langle \partial_i F^0, \partial_j F^0 \rangle,$$

respectively.

Throughout this paper we will make the following assumptions:

- (A1) $F^0 : \bar{\Omega} \longrightarrow \mathbb{R}^3$ is $(\mathcal{C}^2(\bar{\Omega}))^3$, $F^0|_\Omega$ is injective, and its differential dF_ξ^0 is injective $\forall \xi \in \bar{\Omega}$.
- (A2) $a^\varepsilon : \bar{\Omega} \longrightarrow \mathbb{R}$ is $\mathcal{C}^1(\bar{\Omega})$ and $\|a^\varepsilon\|_{L^\infty(\Omega)} \leq \alpha_1$, $\|\nabla a^\varepsilon\|_{L^\infty(\Omega)} \leq \alpha_2/\varepsilon$, where α_1, α_2 are independent of ε .

We note that (A1) and (A2) imply the following consequences:

- (B1) Assumption (A1) implies that $F^0 \in W^{2,\infty}(\Omega)$ (thus $\partial_i F^0, \partial_{ij} F^0 \in L^\infty(\Omega)$).
- (B2) If we denote

$$\lambda(\xi) = \|\partial_1 F^0(\xi) \times \partial_2 F^0(\xi)\|_2,$$

then (A1) implies that there exist $c_1, c_2 > 0$ such that $c_1^0 < \lambda(\xi) < c_2^0 \forall \xi \in \bar{\Omega}$, and we have $n^0(\xi) \in (\mathcal{C}^1(\bar{\Omega}))^3$.

- LEMMA 2.1. *Suppose (A1) and (A2) hold. Then there exist $\varepsilon_0 > 0$ such that $\forall \varepsilon < \varepsilon_0$, $F^\varepsilon|_\Omega$ is injective (see Appendix B for a proof).*

REMARK 2.2. *We will see in section 3 that dF_ξ^ε (which is continuous) is injective $\forall \xi \in \bar{\Omega}$ for $\forall \varepsilon < \varepsilon_0$ for sufficiently small ε_0 . Together with Lemma 2.1, it implies that F^ε is a \mathcal{C}^1 diffeomorphism on Ω .*

2.2. Differential operators on surfaces. In this section we recall some notions of differential geometry that are important for the following. To simplify notation we skip, for now, the ε dependence of the surface. Therefore, let Γ be a surface parameterized by

$$(2.4) \quad \begin{aligned} F : \Omega &\longrightarrow \mathbb{R}^3, \\ (\xi_1, \xi_2) &\longrightarrow (F_1(\xi_1, \xi_2), F_2(\xi_1, \xi_2), F_3(\xi_1, \xi_2)), \end{aligned}$$

where Ω is a bounded subset of \mathbb{R}^2 , $\Gamma \subset \mathbb{R}^3$, and F is $(\mathcal{C}^1(\Omega))^3$. We denote the tangent space at a point $x = F(\xi)$ on the surface by $T_x\Gamma = \text{span}\{\partial_1 F, \partial_2 F\}$, where we suppose that the partial derivatives are linearly independent.

For a point $x = F(\xi)$ of the surface, we consider the two by two matrix $g(\xi) = (g_{ij}(\xi))$, where $g_{ij}(\xi) = \langle \partial_i F(\xi), \partial_j F(\xi) \rangle$ and where $\langle \cdot, \cdot \rangle$ denotes the Euclidean inner product. The first fundamental form of the surface Γ is the restriction of the standard Euclidean inner product on $T_x\Gamma$; i.e., if we denote $X = x_1\partial_1 F + x_2\partial_2 F$ and $Y = y_1\partial_1 F + y_2\partial_2 F$, then

$$(2.5) \quad \begin{aligned} g : T_x\Gamma \times T_x\Gamma &\longrightarrow \mathbb{R}, \\ (X, Y) &\longrightarrow \langle X, Y \rangle = \sum_{ij} x_i y_j g_{ij}, \end{aligned}$$

where $x = F(\xi)$, $g_{ij}(\xi) = \langle \partial_i F(\xi), \partial_j F(\xi) \rangle$ and where $\langle \cdot, \cdot \rangle$ denotes the Euclidean inner product.

REMARK 2.3. *The quadratic form induced by the metric tensor g is positive definite iff $g_{11} > 0$ and $g_{11}g_{22} - g_{12}g_{21} > 0$. The quadratic form given by the first fundamental form (2.5) is symmetric, and $g_{11}g_{22} \geq g_{12}g_{21}$ with strict inequality iff $\partial_1 F, \partial_2 F$ are linearly independent.*

Consider now $u : \Gamma \longrightarrow \mathbb{R}$ to be a $\mathcal{C}^1(\Gamma)$ function defined on the surface, and let $\hat{u}(\xi) = u(F(\xi))$. We define the tangential gradient of u w.r.t. the basis $\{\partial_1 F, \partial_2 F\}$ by

$$(2.6) \quad \nabla_\Gamma u(x) = (\nabla_\xi \hat{u}(\xi))g^{-1},$$

where $x = F(\xi)$. The motivation of this definition is the following. Taking the gradient of $\hat{u}(\xi)$ yields with the chain rule to $\nabla_\xi \hat{u} = \nabla_x u_x (\partial_1 F, \partial_2 F)$, where the last bracket is a three by two matrix (recall that $\partial_i F$ denotes column vectors). We want to define the projection $\nabla_\Gamma u = \nabla_x u|_{T_x\Gamma}$ on the tangent plane $T_x\Gamma$. In the basis of the tangent plane we have $\nabla_\Gamma u = \alpha_1(\partial_1 F)^T + \alpha_2(\partial_2 F)^T$, and we can also write $\nabla_x u = \nabla_\Gamma u + \langle \nabla_x u, n(x) \rangle (n(x))^T$, where $n(x)$ denotes the unit normal vector to the surface at x . Thus since $\langle n(x), \partial_i F \rangle = 0$ we find that

$$\nabla_\xi \hat{u} = \nabla_x u (\partial_1 F, \partial_2 F) = \nabla_\Gamma u (\partial_1 F, \partial_2 F) = (\alpha_1, \alpha_2) g,$$

which yields formula (2.6). The divergence of a tangent vector of the surface $V = v_1\partial_1 F + v_2\partial_2 F$ (the tangential divergence) is then defined by

$$(2.7) \quad \text{div}_\Gamma V = \frac{1}{\sqrt{\det g}} \left(\frac{\partial}{\partial \xi_1} \left(\sqrt{\det g} v_1 \right) + \frac{\partial}{\partial \xi_2} \left(\sqrt{\det g} v_2 \right) \right),$$

and we have the Green formula for a scalar function $u \in \mathcal{C}^1(\Gamma)$ and a tangential vector $V \in (\mathcal{C}^1(\Gamma))^2$

$$(2.8) \quad \int_\Gamma \langle \text{grad}_\Gamma u, V \rangle dx = - \int_\Gamma u \text{div}_\Gamma(V) dx,$$

where we assume that either u or V vanishes at the boundary. Finally, we define the Laplace–Beltrami operator for a function u on the surface by

$$(2.9) \quad \Delta_\Gamma u = \text{div}_\Gamma \nabla_\Gamma u.$$

3. Transformation to a homogenization problem. In this section we will show that the problem (1.2) on the highly oscillating surface Γ^ε can be transformed into an elliptic problem with highly oscillating coefficients on the reference domain Ω (section 3.1). We then further transformed it into a classical homogenization problem (section 3.2). We briefly recall classical homogenization theory and introduce in section 3.3 the heterogeneous multiscale finite element method (HM FEM) on which we build the numerical method used for solving the surface diffusion problem (1.2).

3.1. Ellipticity on the reference domain. For the family of surfaces defined in section 2.1 we consider the weak formulation of problem (1.2).

Problem 1. Find $u^\varepsilon \in H_0^1(\Gamma^\varepsilon)$ such that

$$(3.1) \quad \int_{\Gamma^\varepsilon} \nabla_{\Gamma^\varepsilon} u^\varepsilon (\nabla_{\Gamma^\varepsilon} v)^T dx = \int_{\Gamma^\varepsilon} f v dx \quad \forall v \in H_0^1(\Gamma^\varepsilon),$$

where $f \in H^{-1}(\Gamma^\varepsilon)$.

If we pull back u^ε to the reference domain Ω by $u^\varepsilon(x) = u^\varepsilon(F^\varepsilon(\xi)) = \hat{u}^\varepsilon(\xi)$ and write formally (3.1) in Ω , we obtain the following problem: Find $\hat{u}^\varepsilon \in H_0^1(\Omega)$ such that

$$(3.2) \quad \int_{\Omega} \nabla_\xi \hat{u}^\varepsilon (g^\varepsilon)^{-1} (g^\varepsilon)^{-T} (\nabla_\xi \hat{v})^T \sqrt{\det(g^\varepsilon)} d\xi = \int_{\Omega} \hat{f} \hat{v} \sqrt{\det g^\varepsilon} d\xi \quad \forall \hat{v} \in H_0^1(\Omega),$$

where g^ε is a two by two matrix with coefficients g_{ij}^ε given by (2.3).

The following result states that, under (A1) and (A2) of section 2, the above transformation is well defined and the matrix

$$(3.3) \quad A^\varepsilon = (g^\varepsilon)^{-1} (g^\varepsilon)^{-T} \sqrt{\det g^\varepsilon}$$

is uniformly (in ε and ξ) elliptic and bounded. Hence, under (A1) and (A2), standard elliptic homogenization theory is applicable.

THEOREM 3.1. *Suppose (A1) and (A2) hold; then A^ε is uniformly elliptic and bounded in ε and ξ ; i.e., there exist $\gamma_1, \gamma_2, \varepsilon_0 > 0$ such that $\forall \xi \in \Omega, \forall \eta \in \mathbb{R}^2$, and $\forall \varepsilon 0 < \varepsilon \leq \varepsilon_0$*

$$(3.4) \quad \gamma_1 |\eta|^2 \leq \eta^T A^\varepsilon \eta \leq \gamma_2 |\eta|^2.$$

If $a^\varepsilon(\xi) = a(\xi, \xi/\varepsilon) = a(\xi, y)$ is 1-periodic w.r.t. y_1, y_2 , then $A^\varepsilon(\xi) = A(\xi, \xi/\varepsilon) = A(\xi, y)$ is 1-periodic w.r.t. y_1, y_2 .

We start the proof with some lemmas. We first show that the above transformation is well defined for smooth surfaces.

LEMMA 3.2. *If (A1) holds, then there exist $\beta_1^0, \beta_2^0 > 0$ such that $\forall \xi \in \bar{\Omega}$ and $\forall \eta \in \mathbb{R}^2$ we have*

$$(3.5) \quad \beta_1^0 |\eta|^2 \leq \eta^T g^0 \eta \leq \beta_2^0 |\eta|^2,$$

where g^0 is the two by two matrix with coefficients g_{ij}^0 given by (2.3).

Proof. By (A1), $\partial_1 F^0(\xi)$ and $\partial_2 F^0(\xi)$ are continuous and linearly independent $\forall \xi \in \bar{\Omega}$, and thus (see Remark 2.3) the symmetric matrix g^0 is positive definite $\forall \xi \in \bar{\Omega}$. Since $\bar{\Omega}$ is compact, there exist β_1^0 such that $\forall \xi \in \bar{\Omega}$ and $\forall \eta \in \mathbb{S}^1$ (\mathbb{S}^1 denotes the unit circle), $h(\xi, \eta) = \eta^T g^0(\xi) \eta \geq \beta_1^0 > 0$. Thus, since $h(\xi, \eta)$ is continuous on $\bar{\Omega} \times \mathbb{S}^1$,

$$\eta^T g^0(\xi) \eta \geq \beta_1^0 |\eta|^2 \quad \forall \xi \in \bar{\Omega}, \forall \eta \in \mathbb{R}^2.$$

By the continuity of g^0 on $\bar{\Omega}$ (compact) the right-hand inequality of (3.5) follows. \square

We next discuss the positive definiteness of the quadratic form g^ε .

LEMMA 3.3. *Suppose (A1) and (A2) hold. Then there exist $d_1, \varepsilon_0 > 0$ such that $\forall \xi \in \bar{\Omega}$ and $\forall \varepsilon 0 < \varepsilon \leq \varepsilon_0$*

$$(3.6) \quad g_{11}^\varepsilon = \langle \partial_1 F^\varepsilon, \partial_1 F^\varepsilon \rangle > d_1 > 0.$$

Proof. From the definition of g_{11}^ε we have

$$g_{11}^\varepsilon = g_{11}^0 + 2\varepsilon \langle \partial_1 F^0, \partial_1(a^\varepsilon n^0) \rangle + \varepsilon^2 \langle \partial_1(a^\varepsilon n^0), \partial_1(a^\varepsilon n^0) \rangle.$$

Observe that since $\langle \partial_1 F^0, n^0 \rangle = 0$, we have $\langle \partial_1 F^0, \partial_1(a^\varepsilon n^0) \rangle = \langle \partial_1 F^0, a^\varepsilon \partial_1 n^0 \rangle$, and since $\langle n^0, n^0 \rangle = 1$, we have $\langle \partial_1 n^0, n^0 \rangle = 0$; thus $\langle \partial_1(a^\varepsilon n^0), \partial_1(a^\varepsilon n^0) \rangle = (\partial_1 a^\varepsilon)^2 + (a^\varepsilon)^2 \langle \partial_1 n^0, \partial_1 n^0 \rangle$. Then there is $\varepsilon_0 > 0$ such that

$$(3.7) \quad \begin{aligned} g_{11}^\varepsilon &\geq g_{11}^0 + 2\varepsilon \langle \partial_1 F^0, a^\varepsilon \partial_1 n^0 \rangle \\ &\geq \beta_1^0 - 2\varepsilon \|\partial_1 F^0\|_{L^\infty(\Omega)} \|a^\varepsilon\|_{L^\infty(\Omega)} \|\partial_1 n^0\|_{L^\infty(\Omega)} > d_1 > 0 \quad \forall \varepsilon 0 < \varepsilon \leq \varepsilon_0, \end{aligned}$$

where β_1^0 is given in Lemma 3.2. \square

By the above lemma we have the first condition for positive definiteness (see Remark 2.3). We show next that the second condition also holds uniformly in ε .

LEMMA 3.4. *Suppose (A1) and (A2) hold. Then there exist $d_2, \varepsilon_0 > 0$ such that $\forall \xi \in \bar{\Omega}$ and $\forall \varepsilon 0 < \varepsilon \leq \varepsilon_0$*

$$(3.8) \quad \langle \partial_1 F^\varepsilon, \partial_1 F^\varepsilon \rangle \langle \partial_2 F^\varepsilon, \partial_2 F^\varepsilon \rangle - \langle \partial_1 F^\varepsilon, \partial_2 F^\varepsilon \rangle^2 \geq d_2 > 0.$$

Proof. Define $h^\varepsilon(\xi) = \langle \partial_1 F^\varepsilon, \partial_1 F^\varepsilon \rangle \langle \partial_2 F^\varepsilon, \partial_2 F^\varepsilon \rangle - \langle \partial_1 F^\varepsilon, \partial_2 F^\varepsilon \rangle^2$. By the Cauchy-Schwarz inequality we know that $h^\varepsilon(\xi) \geq 0$, and we also know that $h^\varepsilon(\xi) = 0$ iff $\partial_1 F^\varepsilon$ and $\partial_2 F^\varepsilon$ are collinear $\iff \partial_1 F^\varepsilon \times \partial_2 F^\varepsilon = 0$. We claim that there exists $\varepsilon_0 > 0$ such that $\forall \xi \in \bar{\Omega}$ and $\forall \varepsilon 0 < \varepsilon \leq \varepsilon_0$

$$(3.9) \quad \|\partial_1 F^\varepsilon \times \partial_2 F^\varepsilon\|_2 \geq c > 0.$$

Thus, there exists $d_2 > 0$ such that $h^\varepsilon(\xi) \geq d_2 > 0$, uniformly $\forall \xi \in \bar{\Omega}$ and $\forall \varepsilon 0 < \varepsilon \leq \varepsilon_0$. To prove (3.9), observe that

$$\begin{aligned} &\partial_1 F^\varepsilon \times \partial_2 F^\varepsilon (\partial_1 F^0 + \varepsilon \partial_1(a^\varepsilon) n^0 + \varepsilon a^\varepsilon \partial_1 n^0) \times (\partial_2 F^0 + \varepsilon \partial_2(a^\varepsilon) n^0 + \varepsilon a^\varepsilon \partial_2 n^0) \\ &= \partial_1 F^0 \times \partial_2 F^0 + \varepsilon a^\varepsilon (\partial_1 F^0 \times \partial_2 n^0 + \partial_1 n^0 \times \partial_2 F^0) + \varepsilon^2 (a^\varepsilon)^2 (\partial_1 n^0 \times \partial_2 n^0) + R \\ &=: V + R, \end{aligned}$$

where R contains all terms which are in the tangent plane $T_{F^0(\xi)}\Gamma^0$ and V , which is explicitly given, is orthogonal to the tangent plane $T_{F^0(\xi)}\Gamma^0$. Then there are $\varepsilon_0 > 0$ and $c > 0$ sufficiently small such that $\forall \varepsilon 0 < \varepsilon \leq \varepsilon_0$

$$\begin{aligned} \|\partial_1 F^\varepsilon \times \partial_2 F^\varepsilon\|_2 &\geq \|V\|_2 \geq \|\partial_1 F^0 \times \partial_2 F^0\|_2 \\ &- \varepsilon \|a^\varepsilon\|_{L^\infty(\Omega)} (\|\partial_1 F^0\|_{L^\infty(\Omega)} \|\partial_2 n^0\|_{L^\infty(\Omega)} + \|\partial_1 n^0\|_{L^\infty(\Omega)} \|\partial_2 F^0\|_{L^\infty(\Omega)}) \\ &- \varepsilon^2 \|a^\varepsilon\|_{L^\infty(\Omega)}^2 \|\partial_1 n^0\|_{L^\infty(\Omega)} \|\partial_2 n^0\|_{L^\infty(\Omega)} \geq d_2^0 - \varepsilon c_1 - \varepsilon^2 c_2 \geq c > 0, \end{aligned}$$

where we have used (A1) and the fact that there is $d_2^0 > 0$ such that $\|\partial_1 F^0 \times \partial_2 F^0\|_2 \geq d_2^0 \forall \xi \in \bar{\Omega}$ ($d_2^0 > 0$ exists since $\partial_1 F^0$ and $\partial_2 F^0$ are uniformly (in ξ) linearly independent by Lemma 3.2). \square

Lemmas 3.3 and 3.4, together with the continuity of dF^ε and the injectivity of F^ε shown in Lemma 2.1, give the following corollary.

COROLLARY 3.5. *Suppose (A1) and (A2) hold; then there exists $\varepsilon_0 > 0$ such that $\forall \varepsilon < \varepsilon_0$, F^ε is a C^1 diffeomorphism on Ω . Moreover, there exist c_1, c_2 such that the determinant of the first fundamental form of the surface Γ^ε satisfies $\forall \xi \in \bar{\Omega}$, $\forall \varepsilon 0 < \varepsilon \leq \varepsilon_0$, $c_1 \leq \sqrt{\det g^\varepsilon(\xi)} \leq c_2$. \square*

Using the previous lemmas, we can now prove Theorem 3.1.

Proof of Theorem 3.1. The symmetry is obvious; uniform ellipticity and boundedness follow from Lemmas 3.3 and 3.4. Indeed, observe that if g^ε is uniformly positive definite and bounded, then $(g^\varepsilon)^{-1}$, $(g^\varepsilon)^{-T}$, and $(g^\varepsilon)^{-1}(g^\varepsilon)^{-T}$ are also uniformly positive definite and bounded. By Corollary 3.5 there exist $c_1, c_2 > 0$ such that $c_1 \leq \sqrt{\det g^\varepsilon} \leq c_2$, and thus $A^\varepsilon = (g^\varepsilon)^{-1}(g^\varepsilon)^{-T} \sqrt{\det g^\varepsilon}$ is uniformly elliptic and bounded ($\forall \xi \in \bar{\Omega}$ and $\forall \varepsilon 0 < \varepsilon \leq \varepsilon_0$, where ε_0 is the minimum of the ε_0 defined in Lemmas 3.3 and 3.4).

Now if $a^\varepsilon(\xi) = a(\xi, \xi/\varepsilon) = a(x, y)$ is 1-periodic w.r.t. y_1, y_2 and if we write $F^\varepsilon(\xi) = F(\xi, \xi/\varepsilon) = F(\xi, y)$, then $F(\xi, y), \partial_i F(\xi, y)$ are 1-periodic w.r.t. y_1, y_2 , and since $A^\varepsilon(\xi)$ is a product of functions and inverse functions of the form $\langle \partial_i F^\varepsilon, \partial_j F^\varepsilon \rangle$, $A^\varepsilon(\xi) = A(\xi, \xi/\varepsilon) = A(\xi, y)$ is also 1-periodic w.r.t. y_1, y_2 . \square

Using Lemma 3.2, we can prove similarly the following corollary.

COROLLARY 3.6. *If (A1) holds, then the matrix $A^0 = (g^0)^{-1}(g^0)^{-T} \sqrt{\det g^0}$ is symmetric, continuous, elliptic, and bounded; i.e., there exist γ_1^0, γ_2^0 such that $\forall \xi \in \bar{\Omega}$ and $\forall \eta \in \mathbb{R}^2$*

$$(3.10) \quad \gamma_1^0 |\eta|^2 \leq \eta^T A^0(\xi) \eta \leq \gamma_2^0 |\eta|^2. \quad \square$$

3.2. Reformulation as a homogenization problem. We have in the previous section given sufficient conditions for the reformulation of the surface diffusion problem (3.1) as an elliptic homogenization problem in the parameter domain Ω .

Problem 1b. Find $\hat{u}^\varepsilon \in H_0^1(\Omega)$ such that

$$(3.11) \quad \int_{\Omega} \nabla_{\xi} \hat{u}^\varepsilon A^\varepsilon(\nabla_{\xi} \hat{v})^T d\xi = \int_{\Omega} \hat{f} \hat{v} \sqrt{\det g^\varepsilon} d\xi \quad \forall \hat{v} \in H_0^1(\Omega),$$

where $A^\varepsilon = (g^\varepsilon)^{-1}(g^\varepsilon)^{-T} \sqrt{\det g^\varepsilon}$ and $\hat{f} \in H^{-1}(\Omega)$. We have seen in section 3.1 that under (A1) and (A2), A^ε is uniformly elliptic and bounded for sufficiently small ε . Thus Problem 1b possesses a unique solution by the Lax–Milgram theorem.

REMARK 3.7. *For the more general problem (1.1), we have*

$$A^{\bar{\varepsilon}} = (g^{\bar{\varepsilon}})^{-1} \hat{D}^{\bar{\varepsilon}}(g^{\bar{\varepsilon}})^{-T} \sqrt{\det g^{\bar{\varepsilon}}},$$

where $\hat{D}^{\bar{\varepsilon}}(\xi) = D^{\bar{\varepsilon}}(F^{\bar{\varepsilon}}(\xi))$. Again $A^{\bar{\varepsilon}}$ is uniformly elliptic and bounded for sufficiently small $\bar{\varepsilon} = \max(\bar{\varepsilon}, \varepsilon)$ by Theorem 3.1 and the properties of $D^{\bar{\varepsilon}}$.

If $a^\varepsilon(\xi) = a(\xi, \xi/\varepsilon) = a(x, y)$ is 1-periodic w.r.t. y_1, y_2 and $\varepsilon = n_1 \bar{\varepsilon}$ or $\bar{\varepsilon} = n_2 \varepsilon$ where $n_1, n_2 \in \mathbb{N}$, then $A^{\bar{\varepsilon}}(\xi) = A(\xi, \xi/\bar{\varepsilon}) = A(\xi, \bar{y})$ is also 1-periodic w.r.t. \bar{y}_1, \bar{y}_2 .

We will suppose in what follows that $a^\varepsilon = a(\xi, \xi/\varepsilon) = a(\xi, y)$, where $a(x, y)$ is 1-periodic w.r.t. y_1, y_2 . Observe that the right-hand side of Problem 1b is also oscillating due to the term $\sqrt{\det g^\varepsilon}$. We replace this right-hand side by

$$(3.12) \quad \int_{\Omega} \hat{F} \hat{v} d\xi, \quad \text{with } \hat{F}(\xi) = \hat{f}(\xi) \hat{\mu}(\xi), \quad \hat{\mu}(\xi) = \int_Y \sqrt{\det g(\xi, y)} dy,$$

where $Y = (0, 1)^2$. This is justified by Lemma 3.8 below. Recall (see section 3.1) that $\sqrt{\det g^\varepsilon} \in C^1(\bar{\Omega})$. Thus if $\hat{f} \in L^2(\Omega)$, then $\hat{f} \sqrt{\det g^\varepsilon} \in L^2(\Omega)$, and the following classical result holds (see, for example, [9, Ch. 2.3] for a proof).

LEMMA 3.8. Let $h^\varepsilon(\xi) = \hat{f}(\xi)\sqrt{\det g(\xi, \xi/\varepsilon)}$ be a 1-periodic function in $y = \xi/\varepsilon$. Set $h^\varepsilon(\xi) = h(\xi, \xi/\varepsilon) = h(\xi, y)$. Then

$$(3.13) \quad h^\varepsilon(\xi) \rightharpoonup \hat{F}(\xi) = \int_Y h(\xi, y)dy \quad \text{weakly in } L^2(\Omega),$$

where $Y = (0, 1)^2$.

By the definition of weak convergence (in $L^2(\Omega)$) we have

$$\int_\Omega h^\varepsilon(\xi)\hat{v}d\xi \longrightarrow \int_\Omega \hat{F}\hat{v}d\xi \quad \text{for } \varepsilon \rightarrow 0 \quad \forall \hat{v} \in L^2(\Omega).$$

We will solve numerically the following approximation of Problem 1b.

Problem 2. Find $\hat{w}^\varepsilon \in H_0^1(\Omega)$ such that

$$(3.14) \quad \int_\Omega \nabla_\xi \hat{w}^\varepsilon A^\varepsilon (\nabla_\xi \hat{v})^T d\xi = \int_\Omega \hat{F}\hat{v}d\xi \quad \forall \hat{v} \in H_0^1(\Omega),$$

where $A^\varepsilon = (g^\varepsilon)^{-1}(g^\varepsilon)^{-T}\sqrt{\det g^\varepsilon}$ and \hat{F} is defined in (3.12). The difference between the solutions of Problem 1b and Problem 2 is given by the following lemma.

LEMMA 3.9. Let \hat{u}^ε be the solution of problem (3.11) and \hat{w}^ε be the solution of problem (3.14), where A^ε is uniformly elliptic and bounded and $\hat{f} \in L^2(\Omega)$. Then $\forall \eta > 0$, there exist $\tilde{\varepsilon} > 0$ such that $\forall \varepsilon$ satisfying $0 < \varepsilon < \tilde{\varepsilon}$

$$(3.15) \quad \|\hat{u}^\varepsilon - \hat{w}^\varepsilon\|_{H^1(\Omega)} \leq \frac{\delta(\varepsilon)}{\sqrt{\gamma_1}} \leq \eta,$$

where γ_1 is defined in (3.4) and where

$$(3.16) \quad \delta(\varepsilon) := \left(\sup_{\hat{v} \in L^2(\Omega)} \left| \int_\Omega \left(\hat{f}\sqrt{\det g^\varepsilon} - \hat{F} \right) \hat{v}d\xi \right| \right)^{1/2}.$$

Proof. Since $\hat{f}\sqrt{\det g^\varepsilon} \rightharpoonup \hat{F}$ weakly in $L^2(\Omega)$, $\forall \tilde{\eta} > 0$ there exists $\tilde{\varepsilon}$ such that $\forall \varepsilon$ $0 < \varepsilon < \tilde{\varepsilon}$

$$\left| \int_\Omega \left(\hat{f}\sqrt{\det g^\varepsilon} - \hat{F} \right) \hat{v}d\xi \right| < \tilde{\eta} \quad \forall \hat{v} \in L^2(\Omega),$$

and thus $\delta(\varepsilon)^2 \leq \tilde{\eta}$ $\forall \varepsilon$ $0 < \varepsilon < \tilde{\varepsilon}$.

The lemma follows by noting that $\gamma_1 \|\hat{u}^\varepsilon - \hat{w}^\varepsilon\|_{H^1(\Omega)}^2 \leq B(\hat{u}^\varepsilon - \hat{w}^\varepsilon, \hat{u}^\varepsilon - \hat{w}^\varepsilon) \leq \left| \int_\Omega (\hat{f}\sqrt{\det g^\varepsilon} - \hat{F})(\hat{u}^\varepsilon - \hat{w}^\varepsilon)d\xi \right| \leq \delta(\varepsilon)^2 \leq \tilde{\eta}$ and choosing $\tilde{\eta} = \gamma_1 \eta^2$. \square

3.3. Homogenization problems and the HM FEM. In section 3.3.2 we describe the heterogeneous multiscale method introduced in [11] for homogenization problems such as (3.17). We will then modify it in section 4 for problems such as (3.14), where the right-hand side \hat{F} is not assumed to be analytically available and has to be appropriately sampled. In the HM FEM below, we will study the relation between the multiscale FE solution at positive, small ε and the limiting solution u^0 . Therefore, we briefly review in section 3.3.1 homogenization theory for elliptic problems of the type (3.14).

3.3.1. Homogenization problems. In the bounded parameter domain $\Omega \subset \mathbb{R}^n$ we consider

$$(3.17) \quad -\nabla \cdot (A^\varepsilon(x) \nabla u^\varepsilon) = f(x) \in \Omega, \quad u^\varepsilon = 0 \quad \text{on } \partial\Omega,$$

where we assume that the tensor $A^\varepsilon(x) = A(x, \frac{x}{\varepsilon}) = A(x, y)$ is symmetric, coercive, and 1-periodic w.r.t. each component of y . We further assume that $A_{ij}(x, \cdot) \in L^\infty(\mathbb{R}^n)$ and that $x \rightarrow A_{ij}(x, \cdot)$ is smooth from $\bar{\Omega} \rightarrow L^\infty(\mathbb{R}^n)$. Classical homogenization theory then gives (see, e.g., [5, Ch. 1], [18, Ch. 1.4], [21])

$$(3.18) \quad \|u^\varepsilon - u^0\|_{L^2(\Omega)} \leq C\varepsilon |u^0|_{H^2(\Omega)},$$

where $|\cdot|$ denotes the seminorm, where the solution u^0 of the homogenized problem

$$(3.19) \quad -\nabla \cdot (A^0(x) \nabla u^0) = f(x) \in \Omega, \quad u^0 = 0 \quad \text{on } \partial\Omega,$$

is assumed to belong to $H^2(\Omega)$, and where the homogenized diffusion coefficient A^0 is a smooth matrix given by

$$(3.20) \quad A_{ij}^0(x) = \int_Y \left(A_{ij}(x, y) + \sum_{k=1}^n A_{ik}(x, y) \frac{\partial \chi^j}{\partial y_k}(x, y) \right) dy.$$

Here, $Y = (0, 1)^n$ with $\chi^j(x, \cdot)$ denoting the unique solutions of the cell problems

$$(3.21) \quad \int_Y \nabla \chi^j A \nabla v dy = - \int_Y (Ae_j)^T \nabla v dy \quad \forall v \in W_{per}^1(Y) \quad j = 1, \dots, n,$$

where $(e_j)_{j=1}^n$ is the canonical basis of \mathbb{R}^n and $W_{per}^1(Y) = \{v \in H_{per}^1(Y); \int_Y v dx = 0\}$, where $H_{per}^1(Y)$ is defined as the closure of $\mathcal{C}_{per}^\infty(Y)$ (the subset of $\mathcal{C}^\infty(\mathbb{R}^n)$ of 1-periodic functions) in the H^1 norm. This problem admits a unique solution by the Lax–Milgram theorem. Note that some regularity on $\chi^j(x, \cdot)$ is needed for estimate (3.18) (see [18, Ch. 1.4], [21], [17, Rem. 3.3]).

REMARK 3.10. *By a two-scale ansatz for $u^\varepsilon(x) = u^0(x) + \varepsilon u_1(x, \frac{x}{\varepsilon}) + \mathcal{O}(\varepsilon^2)$, where $u_j(x, y)$ are 1-periodic in the variable y for every $x \in \Omega$, one shows that $u^0(x)$ satisfies (3.19) and that the corrector u_1 is given by*

$$(3.22) \quad u_1(x, y) = \sum_{j=1}^n \chi^j(x, y) \frac{\partial}{\partial x_j} u^0(x),$$

where $\chi^j(x, y)$ are given by (3.21) (see [5, Ch. 1], [18, Ch. 1.4], [9] for details).

3.3.2. HM FEM. Let \mathcal{T}_H be a regular triangulation of $\Omega \subset \mathbb{R}^2$ into shape regular triangles K . We assume in what follows that the mesh \mathcal{T}_H is quasi-uniform of size H . By “macrotriangulation” we mean that H is assumed to be larger than the length scale ε . Let $S_0^1(\Omega, \mathcal{T}_H) \subset H_0^1(\Omega)$ be a corresponding macro FE space defined by

$$(3.23) \quad S_0^1(\Omega, \mathcal{T}_H) = \{u^H \in H_0^1(\Omega); u^H|_K \in \mathcal{P}^1(K) \forall K \in \mathcal{T}_H\},$$

where $\mathcal{P}^1(K)$ is the space of linear polynomials on the triangle K . For a macroelement $K \in \mathcal{T}_H$ we define $K_\varepsilon \subset K$, a sampling subdomain centered at the barycenter of K , usually of size comparable to ε .

The HMM [11] based on the macrospace $S_0^1(\Omega, \mathcal{T}_H)$ is defined by a *modified macrobilinear form*

$$(3.24) \quad B(u^H, v^H) = \sum_{K \in \mathcal{T}_H} \frac{|K|}{|K_\varepsilon|} \int_{K_\varepsilon} \nabla u A(\xi, \xi/\varepsilon) (\nabla v)^T d\xi,$$

where $|K|, |K_\varepsilon|$ denote the measure of K and of K_ε , respectively, and where u is the solution of the following *microproblem*: Find u such that $u - u^H \in W_{per}^1(K_\varepsilon)$ and

$$(3.25) \quad b_{K_\varepsilon}(u, v) = \int_{K_\varepsilon} \nabla u A(\xi_k, \xi/\varepsilon) (\nabla v)^T d\xi = 0 \quad \forall v \in W_{per}^1(K_\varepsilon),$$

where $\xi_k \in K_\varepsilon$. We show in the appendix that the microproblem (3.25) is well posed. Note that the factor $|K|/|K_\varepsilon|$ in (3.24) is a scaling factor which gives the right weight for the macrobilinear form defined on the sampling subdomain K_ε of each macroelement K assuming “uniformity” of the microstructure throughout K .

We then define a variational problem on the macroelement space and approximate the solution of (3.17): Find $u^H \in S_0^1(\Omega, \mathcal{T}_H)$ such that

$$(3.26) \quad B(u^H, v^H) = \langle f, v^H \rangle \quad \forall v^H \in S_0^1(\Omega, \mathcal{T}_H),$$

where $\langle \cdot, \cdot \rangle$ denotes the standard scalar product of L^2 functions. It can be shown that the bilinear form $B(\cdot, \cdot)$ is elliptic and bounded. Thus, the problem (3.26) admits a unique solution. We will discuss it briefly in the appendix, motivate the HM FEM, and obtain, in the periodic setting, error estimates similar to those in [11], [12].

4. Numerical method and error estimates. In this section we will introduce the numerical method based on the HM FEM used to solve the surface problem (1.2) and give error estimates. Recall that we started with the diffusion problem (3.1) on the surface Γ^ε (Problem 1). We then transformed it into a well-posed elliptic problem (3.11) with oscillating coefficients on the parameter domain Ω (Problem 1b). This problem was further transformed in section 3.2 into problem (3.14), obtained by averaging the right-hand side (Problem 2). From now on, we assume that Ω is a convex polygon. Note that this is not a restriction, since we may choose the parameterization F^ε and Ω . We also assume that A^ε defined in (3.3) satisfies $A(\xi, \cdot) \in W^{1,p}(Y)$ ($p > 2$) whenever (3.18) is used (see [17, Rem. 3.3]).

4.1. Numerical method. The numerical method applied to Problem 2 is defined by the following variational problem: Find $\hat{u}^H \in S_0^1(\Omega, \mathcal{T}_H)$ such that

$$(4.1) \quad B(\hat{u}^H, \hat{v}^H) = \langle \hat{F}, \hat{v}^H \rangle \quad \forall \hat{v}^H \in S_0^1(\Omega, \mathcal{T}_H),$$

where

$$(4.2) \quad B(\hat{u}^H, \hat{v}^H) = \sum_{K \in \mathcal{T}_H} \frac{|K|}{|K_\varepsilon|} \int_{K_\varepsilon} \nabla \hat{u} A(\xi_k, \xi/\varepsilon) (\nabla \hat{v})^T d\xi,$$

where ξ_k denotes the barycenter of K , and where \hat{u} is the solution of the microproblem (3.25), and

$$(4.3) \quad \langle \hat{F}, \hat{v}^H \rangle := \sum_{K \in \mathcal{T}_H} \int_K \hat{f}_\mu \hat{v}^H d\xi.$$

REMARK 4.1. *The difference between the above bilinear form and the one defined in (3.24) is that in the matrix A we collocate the slow variable at the barycenter of K . As a consequence the bilinear form is consistent with the homogenized problem (see, e.g., (A.1) in Appendix A).*

To solve the microproblem, a FE space will be used with a triangulation \mathcal{T}_h of mesh-width $h < \varepsilon$ which resolves the small scales in K_ε . Note that since K_ε contains a fixed number of cells, the number of elements in \mathcal{T}_h necessary to resolve the fine scale is independent of ε . The FE space will be described in section 5.1.

4.1.1. Right-hand side computation. Since $\hat{\mu}(\xi_k)$ is not available in closed form, we have to sample it on the microdomain K^ε during the integration process. We show in the following how this can be done without decreasing the order of convergence of the FEM. Observe that if f and $\hat{\mu}$ are smooth we have

$$(4.4) \quad \int_K \hat{f} \hat{\mu} \hat{v}^H d\xi \simeq \hat{f}(\xi_k) \hat{\mu}(\xi_k) \int_K \hat{v}^H d\xi.$$

The sampling of $\hat{\mu}(\xi_k)$ is done in the following way. Let \mathcal{I}_H be an axiparallel mesh of the unit cell $Y = (0, 1)^2$ with congruent rectangles R of size H , and let $\nu(\xi_k, y) := \sqrt{\det(g(\xi_k, y))}$. We define $\hat{\mu}^*(\xi_k) \simeq \hat{\mu}(\xi_k)$ in the following way:

$$(4.5) \quad \hat{\mu}^*(\xi_k) := |R| \sum_{R \in \mathcal{I}_\gamma} \nu(\xi_k, y_R),$$

where y_R is the barycenter of the rectangle R . Note that $\hat{\mu}^*$ can be sampled on K_ε by using the change of variables $y = \xi/\varepsilon$.

LEMMA 4.2. *Suppose that $\nu(\xi_k, \cdot) \in W^{2,2}(Y)$ and that $\xi \rightarrow \nu(\xi, \cdot)$ is continuous from $\bar{\Omega} \rightarrow W^{2,2}(Y)$. Then*

$$(4.6) \quad |\hat{\mu}(\xi_k) - \hat{\mu}^*(\xi_k)| \leq CH^2,$$

where H is the size of the uniform mesh \mathcal{I}_H .

Proof. For the reference rectangle $\tilde{R} = (0, 1)^2$ using the Bramble–Hilbert lemma (see [8, Ch. 4]) standard results give

$$(4.7) \quad |E(\xi_k)| = \left| \int_{\tilde{R}} \tilde{\nu}(\xi_k, \tilde{y}) d\tilde{y} - \tilde{\nu}(\xi_k, \tilde{y}_{\tilde{R}}) \right| \leq C |\tilde{\nu}|_{W^{2,2}(\tilde{R})},$$

since the quadrature scheme is exact for linear polynomials. Furthermore, since $E(\xi)$ is uniformly continuous, the bound is independent of ξ . By a scaling argument $\nu(\xi_k, y) = \tilde{\nu}(\xi_k, F_R(\tilde{y}))$, where $F_R(\tilde{R}) = R$, and summation over all elements, we obtain the stated result. \square

We next estimate the error between the right-hand side (3.14) and its quadrature approximation (4.4).

LEMMA 4.3. *Suppose that $\hat{f} \hat{\mu} \in W^{2,2}(\Omega)$ and that the assumptions of Lemma 4.2 hold. Then*

$$\left| \int_\Omega \hat{f} \hat{\mu} \hat{v}^H d\xi - \sum_{K \in \mathcal{T}_H} |K| \hat{f}(\xi_k) \hat{\mu}^*(\xi_k) \hat{v}^H(\xi_k) \right| \leq CH^2 \|\hat{v}^H\|_{H^1(\Omega)} \quad \forall \hat{v}^H \in S_0^1(\Omega, \mathcal{T}_H).$$

Proof. We have for an element $K \in \mathcal{T}_H$,

$$\begin{aligned} & \left| \sum_{K \in \mathcal{T}_H} \left(\int_K \hat{f} \hat{\mu} \hat{v}^H d\xi - |K| \hat{f}(\xi_k) \hat{\mu}^*(\xi_k) \hat{v}^H(\xi_k) \right) \right| \\ & \leq \left| \sum_{K \in \mathcal{T}_H} \left(\int_K \hat{f} \hat{\mu} \hat{v}^H d\xi - |K| \hat{f}(\xi_k) \hat{\mu}(\xi_k) \hat{v}^H(\xi_k) \right) \right| \\ & \quad + \left| \sum_{K \in \mathcal{T}_H} (|K| \hat{f}(\xi_k) \hat{\mu}(\xi_k) \hat{v}^H(\xi_k) - |K| \hat{f}(\xi_k) \hat{\mu}^*(\xi_k) \hat{v}^H(\xi_k)) \right|. \end{aligned}$$

For the first sum of the right-hand side of the inequality, similar arguments as used in Lemma 4.2 show that it is bounded by $H^2 \|\hat{v}^H\|_{H^1(\Omega)}$ (see [8, Ch. 4]). With the help of Lemma 4.2 we see that each member of the second sum is bounded by $CH^2 \|\hat{v}^H\|_{L^1(K)}$. Summing up over the elements $K \in \mathcal{T}_H$ and using the Cauchy–Schwarz inequality gives the result. \square

Note that the above results are also valid if we sample over triangles in (4.5) instead of quadrilaterals.

4.1.2. Polyhedral mean surfaces. In the procedure described so far for diffusion problems on rough surfaces, we assumed that the surfaces were oscillating over mean surfaces which are smoothly curved. We emphasize, however, that the HM FEM is also applicable when the mean surface is given just by data points which define a polyhedral mean surface. Then, however, the H^1 -error estimates are not valid, since near edges and vertices of the polyhedral midsurface the asymptotic theory of homogenization ceases to be valid.

Since the macrobilinear form is estimated from scale resolved computations on the sampling domains (see section 4.2), for the application of the algorithm we need only the mean surface to be smooth in these subdomains.

4.1.3. Microscale reconstruction. We next discuss how the microscale information (the small scale solution) can be recovered. Following the procedure described in [1], [12], and [23], we extend periodically the known microscale values \hat{u} and define \hat{u}_{rec}^H as

$$(4.8) \quad \hat{u}_{\text{rec}}^H|_K = \hat{u}^H + (\hat{u} - \hat{u}^H)|_K^\sharp,$$

where \hat{u} is the microsolution given by (3.25) and where, for a function $v \in H^1(K_\varepsilon)$, v^\sharp denotes its periodic extension over K defined by

$$v^\sharp(\xi + \varepsilon(l_1, l_2)) = v(\xi) \quad \forall l_1, l_2 \in \mathbb{Z}, \forall \xi \in K_\varepsilon \quad \text{such that } \xi + \varepsilon(l_1, l_2) \in K.$$

Since \hat{u}_{rec}^H can be discontinuous across the macroelement K , we define a broken H^1 norm

$$(4.9) \quad \|u\|_{\bar{H}^1(\Omega)} := \left(\sum_{K \in \mathcal{T}_H} \|\nabla u\|_{L^2(K)}^2 \right)^{1/2}$$

for the error estimates of the reconstructed solution.

4.2. Error estimates on the reference domain Ω . For the convergence results we give in this section, we assume that the numerical method for Problem 2 as described in section 3.2 is applied with exact right-hand side \hat{F} . Lemma 4.3, together with the Strang lemma, shows that the results below are valid with a discretized

right-hand side as discussed in section 4.1. We also assume that the solution of the homogenized solution of Problem 2 is H^2 -regular and that (A1) and (A2) hold for the parameterization of the surface Γ^ε so that with Theorem 3.1 problems (3.11) and (3.14) are well posed. Finally, we assume that the microproblems (3.25) are solved exactly. The case of discretized cell problems for the HMM FEM will be treated elsewhere.

We first have H^1 and L^2 estimates between the HM FEM solution \hat{u}^H of problem (4.1) and \hat{w}^0 , the homogenized solution of Problem 2 (see section 3.2). This is a direct consequence of (A.2) and (A.6) as we show in Appendix A.

THEOREM 4.4. *Let \hat{u}^H be the solution of problem (4.1). Let \hat{w}^0 be the homogenized solution of Problem 2. Then we have*

$$(4.10) \quad \|\hat{w}^0 - \hat{u}^H\|_{H^1(\Omega)} \leq CH \|\hat{F}\|_{L^2(\Omega)},$$

$$(4.11) \quad \|\hat{w}^0 - \hat{u}^H\|_{L^2(\Omega)} \leq CH^2 \|\hat{F}\|_{L^2(\Omega)}.$$

We consider next the L^2 projector P from $H^1(\Omega)$ onto $S_0^1(\Omega, \mathcal{T}_H)$. For $\hat{u} \in H^1(\Omega)$ we define $P\hat{u} \in S_0^1(\Omega, \mathcal{T}_H)$ as the unique solution of the problem

$$(4.12) \quad \langle P\hat{u}, \hat{v}^H \rangle = \langle \hat{u}, \hat{v}^H \rangle \quad \forall \hat{v}^H \in S_0^1(\Omega, \mathcal{T}_H).$$

The error between the projected solutions of Problems 1b and 2, respectively (see (3.11) and (3.14)), and \hat{u}^H is given by the following theorem.

THEOREM 4.5. *Let \hat{u}^H be the solution of problem (4.1). Let $P\hat{u}^\varepsilon, P\hat{w}^\varepsilon$ be the solutions of Problem 1b and 2, respectively, projected by P onto $S_0^1(\Omega, \mathcal{T}_H)$. Then we have*

$$(4.13) \quad \|P\hat{w}^\varepsilon - \hat{u}^H\|_{L^2(\Omega)} \leq C(\varepsilon + H^2) \|\hat{F}\|_{L^2(\Omega)},$$

$$(4.14) \quad \|P\hat{u}^\varepsilon - \hat{u}^H\|_{L^2(\Omega)} \leq C(\varepsilon + H^2) \|\hat{F}\|_{L^2(\Omega)} + \delta(\varepsilon),$$

$$(4.15) \quad \|P\hat{w}^\varepsilon - \hat{u}^H\|_{H^1(\Omega)} \leq C(\varepsilon/H + H) \|\hat{F}\|_{L^2(\Omega)},$$

$$(4.16) \quad \|P\hat{u}^\varepsilon - \hat{u}^H\|_{H^1(\Omega)} \leq C(\varepsilon/H + H) \|\hat{F}\|_{L^2(\Omega)} + \delta(\varepsilon),$$

where $\delta(\varepsilon) \rightarrow 0$ for $\varepsilon \rightarrow 0$ is as in Lemma 3.9.

Proof. Estimates (4.13) and (4.15) follow from (A.9) and (A.10) of Appendix A, respectively. Estimates (4.14) and (4.16) follow from (4.13) and (4.15), respectively, Lemma 3.9, the triangle inequality, and the following bound for the L^2 projection onto the FE space in convex polygonal domains (see [6, Cor. 7.8, p. 91]):

$$\|P\hat{w}^\varepsilon - P\hat{u}^\varepsilon\|_{H^1(\Omega)} \leq C \|\hat{w}^\varepsilon - \hat{u}^\varepsilon\|_{H^1(\Omega)}. \quad \square$$

Next we have L^2 estimates between the solutions of Problems 1b and 2 and the numerical solution \hat{u}^H .

THEOREM 4.6. *Let \hat{u}^H be the solution of problem (4.1). Let $\hat{u}^\varepsilon, \hat{w}^\varepsilon$ be the solutions of Problem 1b and 2, respectively. Then we have*

$$(4.17) \quad \|\hat{w}^\varepsilon - \hat{u}^H\|_{L^2(\Omega)} \leq C(\varepsilon + H^2) \|\hat{F}\|_{L^2(\Omega)},$$

$$(4.18) \quad \|\hat{u}^\varepsilon - \hat{u}^H\|_{L^2(\Omega)} \leq C(\varepsilon + H^2) \|\hat{F}\|_{L^2(\Omega)} + \delta(\varepsilon),$$

where $\delta(\varepsilon) \rightarrow 0$ for $\varepsilon \rightarrow 0$ is as in Lemma 3.9.

Proof. Estimation (4.17) follows from (A.7) of Appendix A, and (4.18) follows from (4.17), Lemma 3.9, and the triangle inequality. \square

Finally, we give error estimates between the reconstructed numerical solution \hat{u}_{rec}^H as defined in (4.8) and the solutions of Problem 1b and 2.

THEOREM 4.7. *Let \hat{u}_{rec}^H be the reconstructed solution (as defined in (4.8)) of problem (4.1). Let $\hat{u}^\varepsilon, \hat{w}^\varepsilon$ be the solutions of Problem 1b and 2, respectively. Then we have*

$$(4.19) \quad \|\hat{w}^\varepsilon - \hat{u}_{\text{rec}}^H\|_{\bar{H}^1(\Omega)} \leq C(\sqrt{\varepsilon} + H)\|\hat{F}\|_{L^2(\Omega)},$$

$$(4.20) \quad \|\hat{u}^\varepsilon - \hat{u}_{\text{rec}}^H\|_{\bar{H}^1(\Omega)} \leq C(\sqrt{\varepsilon} + H)\|\hat{F}\|_{L^2(\Omega)} + \delta(\varepsilon),$$

where $\delta(\varepsilon) \rightarrow 0$ for $\varepsilon \rightarrow 0$ is as in Lemma 3.9 and $\bar{H}^1(\Omega)$ denotes the broken H^1 norm defined in (4.9).

Proof. Estimation (4.19) is given by (A.8) of Appendix A, and (4.20) follows from (4.19), Lemma 3.9, and the triangle inequality. \square

4.3. Pullback and error estimates on the surface. We will give in this section error estimates on the surface Γ^ε . We first give a pullback lemma which will allow us to shift the error estimates of section 4.2 onto the surface Γ^ε .

LEMMA 4.8. *Suppose (A1) and (A2) hold. Let $u(x) = u(F^\varepsilon(\xi)) = \hat{u}(\xi)$. Then $u(x) \in H^1(\Gamma^\varepsilon) \iff \hat{u} \in H^1(\Omega)$, and there exist $0 < \beta_1 < \beta_2 < \infty$ such that $\forall \varepsilon \ 0 < \varepsilon \leq \varepsilon_0$*

$$(4.21) \quad \beta_1 \|\hat{u}\|_{H^1(\Omega)} \leq \|u\|_{H^1(\Gamma^\varepsilon)} \leq \beta_2 \|\hat{u}\|_{H^1(\Omega)}.$$

Proof. Recall that if (A1) and (A2) hold, $F^\varepsilon(\xi)$ is a diffeomorphism for all sufficiently small $\varepsilon < \varepsilon_0$. Suppose $u(x) \in H^1(\Gamma^\varepsilon)$; then the correspondence $u(x) = u(F^\varepsilon(\xi)) = \hat{u}(\xi)$ uniquely defines \hat{u} . We have seen that $\nabla_{\Gamma^\varepsilon} u(x) = \nabla_\xi \hat{u}(\xi)(g^\varepsilon(\xi))^{-1}$ (see (2.6)), where g^ε is defined in (2.3) and

$$\int_{\Gamma^\varepsilon} \nabla_{\Gamma^\varepsilon} u (\nabla_{\Gamma^\varepsilon} u)^T dx = \int_{\Omega} \nabla_\xi \hat{u} (g^\varepsilon)^{-1} (g^\varepsilon)^{-T} (\nabla_\xi \hat{u})^T \sqrt{\det g^\varepsilon} d\xi.$$

Since $A^\varepsilon(\xi) = (g^\varepsilon(\xi))^{-1} (g^\varepsilon(\xi))^{-T} \sqrt{\det g^\varepsilon(\xi)}$ is uniformly elliptic and bounded (see Theorem 3.1) we have

$$\gamma_1 \|\nabla \hat{u}\|_{L^2(\Omega)} \leq \|\nabla u\|_{L^2(\Gamma^\varepsilon)} \leq \gamma_2 \|\nabla \hat{u}\|_{L^2(\Omega)}.$$

Similarly we also have (note that $\sqrt{\det g^\varepsilon}$ is uniformly bounded; see Corollary 3.5)

$$c_1 \|\hat{u}\|_{L^2(\Omega)} \leq \|u\|_{L^2(\Gamma^\varepsilon)} \leq c_2 \|\hat{u}\|_{L^2(\Omega)}.$$

We have shown that $\hat{u} \in H^1(\Omega)$ and that (4.21) holds. Similarly, if $\hat{u} \in H^1(\Omega)$, then $u \in H^1(\Gamma^\varepsilon)$, where $u(x) = \hat{u}((F^\varepsilon)^{-1}(x))$, and the proof is complete. \square

Let u^ε be the solution of (3.1). Let further $w^\varepsilon, w^0, Pw^\varepsilon, u^H, u_{\text{rec}}^H$ be the functions considered in section 4.2 lifted on the surface Γ^ε ; i.e., for a function \hat{v} given on Ω we define v on Γ^ε by

$$(4.22) \quad v(x) = v(F^\varepsilon(\xi)) := \hat{v}(\xi).$$

The pullback lemma, Lemma 4.8, shows that Theorems 4.4–4.7 with obvious changes are also valid on the surface Γ^ε for $\hat{w}^\varepsilon, \hat{w}^0, \hat{P}w^\varepsilon, \hat{u}^H, \hat{u}_{\text{rec}}^H$ lifted on the surface by (4.22).

Finally, the following theorem shows that the solution of Problem 2 lifted on the surface Γ^ε converges to the solution of Problem 1 for $\varepsilon \rightarrow 0$. Thus, the numerical method (applied to Problem 2) is consistent with the original problem.

THEOREM 4.9. *Let u^ε be the solution of Problem 1 (see (3.1)). Let w^ε, w^0 be the solutions of Problem 2 (see (3.14)) and its homogenized version, respectively, lifted on the surface Γ^ε by (4.22). Then we have*

$$(4.23) \quad \|w^\varepsilon - w^0\|_{H^1(\Gamma^\varepsilon)} \leq C\varepsilon \|\hat{F}\|_{L^2(\Omega)},$$

$$(4.24) \quad \|u^\varepsilon - w^\varepsilon\|_{H^1(\Gamma^\varepsilon)} \leq C\delta(\varepsilon),$$

where $\delta(\varepsilon) \rightarrow 0$ for $\varepsilon \rightarrow 0$ is as in Lemma 3.9.

Proof. With the pullback lemma, Lemma 4.8, estimations (4.23) and (4.24) follow from (3.18) and Lemma 3.9, respectively. \square

COROLLARY 4.10.

$$(4.25) \quad \|u^\varepsilon - w^0\|_{H^1(\Gamma^\varepsilon)} \leq C(\varepsilon \|\hat{F}\|_{L^2(\Omega)} + \delta(\varepsilon)).$$

5. Implementational aspects and numerical examples. We first explain in section 5.1 implementation aspects concerning the scales coupling in the HM FEM. We then discuss in section 5.2 the application of the proposed algorithm to several examples.

5.1. Weak scale coupling through Lagrange multipliers. The definition of the macrobilinear form (4.2) is based on the solution of the microproblems (3.25). These problems have to be solved on a micro FE space of ε -periodic functions $S_{per}^1(K_\varepsilon, \mathcal{T}_h)$, which is a finite dimensional subspace of $W_{per}^1(K_\varepsilon)$ defined in section 3.3. \mathcal{T}_h is a quasi-uniform quadrilateral mesh of the sampling domain K_ε chosen to resolve the ε -scale. The sampling domain is defined as $K_\varepsilon = \xi_k + \varepsilon(-1/2, 1/2)^2$, where ξ_k is at the barycenter of the macroelement K . As already noted, the number of elements in \mathcal{T}_h necessary to resolve the fine scale is independent of ε , since K_ε contains a fixed number of cells.

5.1.1. Macrostiffness matrix. Let $\hat{u}^H = \sum_{i=1}^N \zeta_i \varphi_i^H$ be the (unknown) solution of problem (4.1), where $\{\varphi_i^H\}_{i=1}^N$ is a basis of $S_0^1(\Omega, \mathcal{T}_H)$. As usual in an element-oriented approach, for each element $K \in \mathcal{T}_H$ we select $N_K \in S_0^1(\Omega, \mathcal{T}_H)$, the nodal basis functions associated with the vertices of K , and we compute the element contribution to the stiffness matrix of the bilinear form (4.2). That is, we compute the matrix A_K whose entries are given, for $\varphi_l^H, \varphi_p^H \in N_K$, by

$$(5.1) \quad A_{lp}(\varphi_l^H, \varphi_p^H) = \frac{|K|}{|K_\varepsilon|} \int_{K_\varepsilon} \nabla \varphi_l^h \cdot A(\xi_k, \xi_k/\varepsilon) \nabla \varphi_p^h d\xi = (\alpha^l)^T B_{K_\varepsilon} \alpha^p,$$

where $K_\varepsilon \subset K$, $\varphi_l^h = \sum_{i=1}^n \alpha_i^l \psi_i^h$, $\varphi_p^h = \sum_{i=1}^n \alpha_i^p \psi_i^h$, $\{\psi_i^h\}_{i=1}^n$ is a basis of the micro FE space (5.4) defined below, and B_{K_ε} is the microstiffness matrix (5.10) also defined below.

The functions φ_l^h, φ_p^h are computed on the microsampling domain K_ε as explained in the following. Note that we used the notations $\alpha^l = (\alpha_1^l, \dots, \alpha_n^l)^T$, $\alpha^p = (\alpha_1^p, \dots, \alpha_n^p)^T$.

5.1.2. Saddle point problem and microstiffness matrix. We denote by φ^H one element of the macronodal basis of the macroelement K and by φ^h its corresponding microfunction, which is defined by the following problem (see section 4.1 and Appendix A): Find φ^h such that $(\varphi^h - \varphi^H) \in S_{per}^1(K_\varepsilon, \mathcal{T}_h)$ and

$$(5.2) \quad \int_{K_\varepsilon} \nabla \varphi^h A(\xi_k, \xi/\varepsilon) (\nabla \phi)^T d\xi = 0 \quad \forall \phi \in S_{per}^1(K_\varepsilon, \mathcal{T}_h),$$

where

$$(5.3) \quad S_{per}^1(K_\varepsilon, \mathcal{T}_h) = \{u^h \in W_{per}^1(K_\varepsilon); u^h|_T \in \mathcal{P}^1(T), T \in \mathcal{T}_h\},$$

where $\mathcal{P}^1(K)$ is the space of linear polynomials on the triangle T (we could have also chosen the space of bilinear polynomials, for example, for the micro FE space).

To avoid having to impose periodic essential boundary conditions on the micro FE space, we transform this into a saddle point problem over the space

$$(5.4) \quad S^1(K_\varepsilon, \mathcal{T}_h) = \{u^h \in H^1(K_\varepsilon); u^h|_T \in \mathcal{P}^1(T), T \in \mathcal{T}_h\}$$

with a basis defined by $\{\psi_i^h\}_{i=1}^n$.

In the following we show how the periodic boundary conditions (and hence the scale coupling) can be weakly enforced through Lagrange multipliers. We write (5.2) as a minimization problem

$$(5.5) \quad \min \frac{1}{2} \int_{K_\varepsilon} \nabla \varphi^h A(\xi_k, \xi/\varepsilon) (\nabla \varphi^h)^T d\xi$$

over all functions $\varphi^h \in S^1(K_\varepsilon, \mathcal{T}_h)$ satisfying $\varphi^h - \varphi^H \in S_{per}^1(K_\varepsilon, \mathcal{T}_h)$.

To define the constraints functional, we introduce the following notation. Let $S^1(\partial K_\varepsilon, \mathcal{T}_{\partial,h})$ be a linear FE space defined on the boundary ∂K_ε with a basis given by $(\vartheta_i^h)_{i=1}^{2m}$. Furthermore, we order this basis such that the first m nodes p_i are on two edges of ∂K_ε which intersect. For a node p_i we denote by $p_{\sigma(i)}$ the node on the opposite edge by mirror symmetry. The constraints functional is then defined by $G(\varphi^h - \varphi^H, \vartheta, \kappa) = 0$ with G given by

$$(5.6) \quad G(\psi, \vartheta, \kappa) = \sum_{i=1}^m \left(\psi(p_i) - \psi(p_{\sigma(i)}) \right) \vartheta(p_i) + \kappa \int_{K_\varepsilon} \psi d\xi,$$

where $\vartheta \in S^1(\partial K_\varepsilon, \mathcal{T}_{\partial,h})$, $\psi \in S^1(K_\varepsilon, \mathcal{T}_h)$, and $\kappa \in \mathbb{R}$.

The constraints functional allows us to define the Lagrangian (see [6, Ch. 4]). Computing the variation of the Lagrangian leads to the following saddle point problem: Find $\varphi^h \in S^1(K_\varepsilon, \mathcal{T}_h)$ and $\vartheta_0 \in S^1(\partial K_\varepsilon, \mathcal{T}_{\partial,h})$, $\kappa_0 \in \mathbb{R}$ such that

$$(5.7) \quad \int_{K_\varepsilon} \nabla \varphi^h A(\xi_k, \xi/\varepsilon) (\nabla \psi)^T d\xi + G(\psi, \vartheta_0, \kappa_0) = 0 \quad \forall \psi \in S^1(K_\varepsilon, \mathcal{T}_h),$$

$$G(\varphi^h - \varphi^H, \vartheta, \kappa) = 0 \quad \forall \vartheta \in S^1(\partial K_\varepsilon, \mathcal{T}_{\partial,h}), \forall \kappa \in \mathbb{R}.$$

Writing $\varphi^h = \sum_{i=1}^n \alpha_i \psi_i^h$, $\varphi^H = \sum_{i=1}^n \beta_i \psi_i^h$, and $\vartheta_0 = \sum_{i=1}^{2m} \lambda_i \vartheta_i^h$ we are led to the linear system

$$(5.8) \quad B_{K_\varepsilon} \alpha + D^T \lambda = 0,$$

$$(5.9) \quad D(\alpha - \beta) = 0,$$

where $\lambda = (\kappa_0, \lambda_1, \dots, \lambda_m)^T \in \mathbb{R}^{m+1}$, D is the $(m+1) \times n$ matrix of the constraints (where m is the number of nodes of the mesh $\mathcal{T}_{\partial,h}$), and B_{K_ε} is the $n \times n$ microstiffness matrix corresponding to the microvariational problem (5.7) whose entries are given by

$$(5.10) \quad (B_{K_\varepsilon})_{ij} = \int_{K_\varepsilon} \nabla \psi_i A(\xi_k, \xi/\varepsilon) (\nabla \psi_j)^T d\xi.$$

We emphasize that with this procedure we could enforce *other boundary conditions* for coupling the scales just by modifying the Lagrangian functional (5.6).

5.2. Numerical examples. We give here several examples to illustrate the performance of the proposed numerical method on surfaces: As explained in section 3.2, we will transform the problem on the surface to a corresponding problem on the reference domain (3.11). For this problem we compute a numerical reference solution via scale resolution, i.e., by a standard FEM with an “overkill” mesh that fully resolves (with a large number of degrees of freedom) the fine scales of the solution. The HM FEM is then applied to the problem on the reference domain with a smooth right-hand side (see (3.14)). We compare next the L^2 projection of the reference solution with the numerical solution in the L^2 norm and the H^1 norm, and we compute an error estimate on the reference domain Ω . By the results of section 4.3, similar estimates holds on the physical surface Γ^ε . In the following, we take a sufficiently small micromesh in order to avoid the influence of the discretized small scale FEM on the macrosolution. As already noted, this influence will be studied elsewhere.

Example 1. We take the surface given by (see Figure 5.1)

$$F^\varepsilon(\xi_1, \xi_2) = \underbrace{(\xi_1, \xi_2, \xi_1(1 - \xi_1))}_{F^0} + \varepsilon \sin 2\pi\xi_1/\varepsilon \cdot n(\xi_1, \xi_2),$$

where $(\xi_1, \xi_2) \in \Omega = (0, 1)^2$ and where $n^0(\xi) = \frac{(\frac{\partial F^0(\xi)}{\partial \xi_1} \times \frac{\partial F^0(\xi)}{\partial \xi_2})}{\|\frac{\partial F^0(\xi)}{\partial \xi_1} \times \frac{\partial F^0(\xi)}{\partial \xi_2}\|} = \frac{(2\xi_1 - 1, 0, 1)}{\sqrt{(2\xi_1 - 1)^2 + 1}}$. We then have

$$g^\varepsilon = \begin{pmatrix} a^2 + b^2 & 0 \\ 0 & 1 \end{pmatrix}$$

and

$$A^\varepsilon = (g^\varepsilon)^{-1} (g^\varepsilon)^{-T} \sqrt{\det g^\varepsilon} = \begin{pmatrix} (a^2 + b^2)^{-3/2} & 0 \\ 0 & (a^2 + b^2)^{1/2} \end{pmatrix},$$

where

$$a = 1 + \cos(2\pi\xi_1/\varepsilon)n_1^0(\xi) + 2\pi\varepsilon \sin(2\pi\xi_1/\varepsilon) \frac{\partial n_1^0}{\partial \xi_1},$$

$$b = 1 - 2\xi_1 + \cos(2\pi\xi_1/\varepsilon)n_3^0(\xi) + 2\pi\varepsilon \sin(2\pi\xi_1/\varepsilon) \frac{\partial n_3^0}{\partial \xi_1},$$

and $n_i^0(\xi)$ denotes the component of the normal vector $n^0(\xi)$. The problem that we solve is then

$$\begin{aligned} -\Delta_{\Gamma_\varepsilon} u^\varepsilon &= f \text{ on } \Gamma^\varepsilon, \\ u^\varepsilon|_{\partial\Gamma_D^\varepsilon} &= 0, \\ n \cdot \nabla_{\Gamma_\varepsilon} u^\varepsilon|_{\partial\Gamma_N^\varepsilon} &= 0, \end{aligned}$$

where n denotes the normal to the surface Γ^ε , $f = 1$, and

$$\partial\Gamma_D^\varepsilon := \{F^\varepsilon(\xi_1, \xi_2); (\xi_1, \xi_2) \in \{\xi_1 = 0\} \cup \{\xi_1 = 1\}\} \quad \text{and} \quad \partial\Gamma_N^\varepsilon := \partial\Gamma_\varepsilon \setminus \partial\Gamma_D^\varepsilon.$$

We derive the corresponding problem on the reference domain with a smooth right-hand side (see (3.14)) which will be used to derive the HM FEM: Find $w^\varepsilon \in H_D^1(\Omega)$ such that

$$\int_\Omega \nabla_\xi \hat{w}^\varepsilon A^\varepsilon (\nabla_\xi \hat{v})^T d\xi = \int_\Omega \hat{F} \hat{v} d\xi \quad \forall \hat{v} \in H_D^1(\Omega),$$

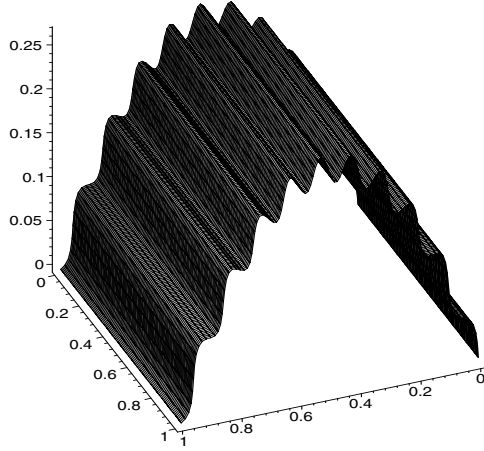


FIG. 5.1. Γ_ε for Example 1 ($\varepsilon = 1/10$).

where $\hat{F} = \hat{f}\hat{\mu}(\xi)$, $\hat{\mu}(\xi) = \int_Y \sqrt{\det(g(\xi, y))} dy$, $Y = (0, 1)^2$, and

$$H^1_{\hat{D}}(\Omega) := \{\hat{v} \in H^1(\Omega); \hat{v}|_{\partial\Omega_D} = 0\} \quad \text{and} \quad \partial\Omega_{\hat{D}} := \{(\xi_1, \xi_2); F_\varepsilon(\xi_1, \xi_2) \in \partial\Gamma_D\}.$$

We apply the HM FEM to the above problem, and we give in Table 5.1 and in Figure 5.2 the results for $\varepsilon = 1/10$ for which we have 10 periods of oscillation in the surface Γ^ε . The reference solution was computed via scale resolution on a 101×101 mesh (9801 degrees of freedom). We present the results for macromesh refinement.

TABLE 5.1
Convergence for Example 1 on Ω for $\varepsilon = 1/10$.

Macrosizes	L^2	H^1
1/2	0.110250	0.381956
1/4	0.027403	0.148241
1/8	0.006064	0.088747

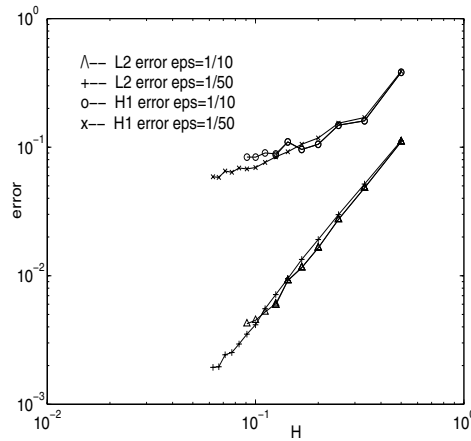


FIG. 5.2. Convergence for Example 1.

We next repeat the experiment but decrease ε to $1/50$ so that there are now 50 periods of oscillation in the surface Γ_ε . The reference solution was computed via scale resolution on a 501×501 mesh (249001 degrees of freedom). Again, we present the errors and convergence rates in Table 5.2 and in Figure 5.2, respectively, for macromesh refinement.

TABLE 5.2
Convergence for Example 1 on Ω for $\varepsilon = 1/50$.

Macrosize	L^2	H^1
1/2	0.112202	0.388681
1/4	0.029885	0.153641
1/8	0.007130	0.083965
1/16	0.001938	0.058880

In view of Theorem 4.5 we expect two sources of error: the consistency error introduced by the smooth right-hand side and the discretization error of the numerical method. We see in Tables 5.1 and 5.2 and in Figure 5.2 an H^2 rate of convergence in the L^2 norm and an H rate of convergence in the H^1 norm. As predicted, the HM FEM captures the correct macroscale behavior of the solution with a number of degrees of freedom which is independent of the scale parameter ε (for $H \simeq \varepsilon$ a resonance error seems to occur for the H^1 norm but not for the L^2 norm as indicated by Theorem 4.5).

Example 2. We take the surface given by (see Figure 5.3)

$$F^\varepsilon(\xi_1, \xi_2) = \underbrace{(\xi_1, \xi_2, \xi_1(1 - \xi_1) + \xi_2(1 - \xi_2))}_{F^0} + \varepsilon(\sin 2\pi\xi_1/\varepsilon + \sin 2\pi\xi_2/\varepsilon) \cdot n^0(\xi_1, \xi_2),$$

where $(\xi_1, \xi_2) \in \Omega^\varepsilon = (0, 1)^2$ and where $n(\xi) = \frac{(\frac{\partial F^0(\xi)}{\partial \xi_1} \times \frac{\partial F^0(\xi)}{\partial \xi_2})}{\|\frac{\partial F^0(\xi)}{\partial \xi_1} \times \frac{\partial F^0(\xi)}{\partial \xi_2}\|} = \frac{(2\xi_1 - 1, 2\xi_2 - 1, 1)}{\sqrt{(2\xi_1 - 1)^2 + (2\xi_2 - 1)^2 + 1}}$. Here g^ε is no longer diagonal but is a full (symmetric) matrix. The problem that we solve is then

$$\begin{aligned} -\Delta_{\Gamma_\varepsilon} u^\varepsilon &= f \text{ on } \Gamma^\varepsilon, \\ u^\varepsilon|_{\partial\Gamma^\varepsilon} &= 0, \end{aligned}$$

where $f = 1$.

We derive the corresponding problem on the reference domain with a smooth right-hand side (see (3.14)) on which we apply the HM FEM. We give in Table 5.3 and in Figure 5.4 the results for $\varepsilon = 1/10$ for which we have 10 periods of oscillation in the surface Γ^ε . The reference solution was computed via scale resolution on a 101×101 mesh (9801 degrees of freedom).

We next decrease ε to $1/50$ for which we have 50 periods of oscillation in the surface Γ_ε and give in Table 5.4 and in Figure 5.4 the results for macromesh refinement. The reference solution was computed via scale resolution on a 501×501 mesh (249001 degrees of freedom).

We see in Tables 5.3 and 5.4 and in Figure 5.4 that we have an $(H)^2$ rate of convergence for the L^2 norm and a convergence rate better than H for the H^1 norm. Again the method is able to capture the right macroscale behavior with substantially fewer degrees of freedom than the standard FEM, and the errors are independent of ε (again for $H \simeq \varepsilon$ a resonance error seems to occur for the H^1 norm but not for the L^2 norm as indicated by Theorem 4.5).

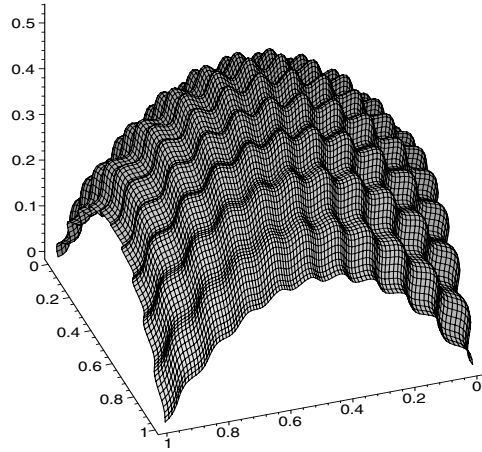


FIG. 5.3. Γ_ε for Example 2 ($\varepsilon = 1/10$).

TABLE 5.3
Convergence for Example 2 on Ω for $\varepsilon = 1/10$.

Macrosizes	L^2	H^1
1/2	0.067495	0.381811
1/4	0.026775	0.148096
1/8	0.005386	0.048682

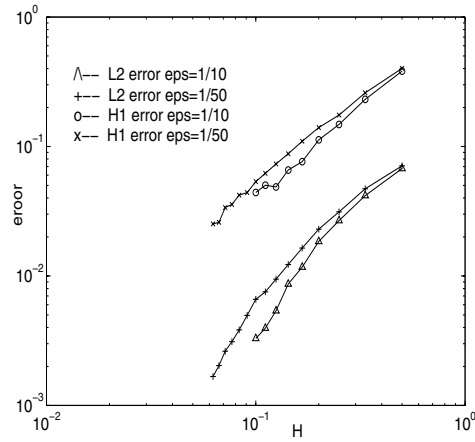


FIG. 5.4. Convergence for Example 2.

TABLE 5.4
Convergence for Example 2 on Ω for $\varepsilon = 1/50$.

Macrosizes	L^2	H^1
1/2	0.070888	0.401007
1/4	0.031271	0.174734
1/8	0.009449	0.073331
1/16	0.001673	0.025217

Example 3. We take the same surface Γ^ε as in Example 2, and we add an anisotropic tensor; i.e., we consider the problem

$$(5.11) \quad \begin{aligned} -\nabla_{\Gamma^\varepsilon} \cdot (D^{\tilde{\varepsilon}} \nabla_{\Gamma^\varepsilon} u) &= f \in \Gamma^\varepsilon, \\ u &= 0 \text{ on } \partial\Gamma^\varepsilon, \end{aligned}$$

where $f = 1$ and $D^{\tilde{\varepsilon}}$ is given (in the parameter domain) by

$$\begin{pmatrix} \sin 2\pi\xi_1/\tilde{\varepsilon} + 2 & 0 \\ 0 & \sin 2\pi\xi_2/\tilde{\varepsilon} + 2 \end{pmatrix}.$$

As in the previous example, we derive the corresponding problem on the reference domain with a smooth right-hand side on which we will apply the numerical method. We first choose $\tilde{\varepsilon} = \varepsilon = 1/50$ and give in Table 5.5 the convergence results. We see that the rate of convergence for the L^2 norm is faster than linear, that the rate of convergence for the H^1 norm is linear, and that the performance is independent of ε . By Remark 3.7, Theorem 4.5 is still valid for this case. We next choose $\tilde{\varepsilon} = 2\varepsilon = 2/50$ and give in Table 5.6 the convergence results. The microdomains $K_{\tilde{\varepsilon}}$ are of measure $|K_{\tilde{\varepsilon}}| = \tilde{\varepsilon}^2$. We have a similar convergence rate as before. Note that Theorem 4.5 is still valid if $\varepsilon = n_1\tilde{\varepsilon}$ or $\tilde{\varepsilon} = n_2\varepsilon$, where $n_1, n_2 \in \mathbb{N}$, provided we choose $\max\{\varepsilon, \tilde{\varepsilon}\}$ as the patch size of the cell problem.

TABLE 5.5
Convergence for Example 3 on Ω for $\varepsilon = \tilde{\varepsilon} = 1/50$.

Macrosizes	L^2	H^1
1/2	0.039907	0.225747
1/4	0.017713	0.098793
1/8	0.005440	0.042883

TABLE 5.6
Convergence for Example 3 on Ω for $\varepsilon = 1/50$, $\tilde{\varepsilon} = 2/50$.

Macrosizes	L^2	H^1
1/2	0.040445	0.228794
1/4	0.018229	0.101511
1/8	0.005911	0.046000

6. Conclusions and perspectives. We have shown how diffusion problems on rough surfaces can be handled in the framework of elliptic homogenization and solved numerically with HM FEMs with accuracy and complexity that are scale independent. The transformation to the reference domain, i.e., Theorem 3.1, has been proved under (A1) and (A2) and is also valid if the oscillating coefficient a^ε is not periodic.

We have shown in our implementation how the microproblems can be solved in nonperiodic FE spaces by enforcing weakly the periodicity through Lagrange multipliers. This allows for general nonperiodic meshes in the micro FE space.

In application, it is sometimes more realistic to assume that a^ε is random. Results for the heterogeneous multiscale FE scheme described in section 3.3.2 (i.e., for nonoscillating source terms) have been given for the random case (for stationary ergodic random fields) in [12]. It is shown that the rate of convergence depends on the size of the microdomains (this dependency has been characterized in one dimension). It thus seems possible to extend the method given in this paper for problems on surfaces with random oscillations.

In the present paper we treated problems which are parameterized by one chart and a C^1 map F^ε . This is not possible for all surfaces, and, in general, one should use an atlas of charts. It is explained in [15] how to construct such an atlas approximating a triangulated surface. This could be used to adapt the method we have proposed for more general surfaces. An approximation of the midsurface Γ by a polyhedral interpolant Γ_H is not considered here but is often the only available representation of Γ from, e.g., experimental data. The additional error introduced by such surface approximations into the bilinear forms could be analyzed within the present framework, under suitable assumptions on the measured data.

Appendix A. The HM FEM and error estimates. We briefly discuss in this appendix the existence and uniqueness of a solution for the HMM FEM. We also explain the relation of the modified bilinear form (4.1) for solving (3.17) and the homogenized problem (3.19) and give some convergence results we used in our analysis for surface diffusion problems. The convergence results given here are along the lines of [11], [12] (some of them, such as estimations (A.2) and (A.6), in an improved form). We recall that we assume that the microproblems (3.25) are solved exactly. We also assume that Ω is a convex polygon, that the assumptions of section 3.3.1 hold, and that A^ε satisfies $A(\xi, \cdot) \in W^{1,p}(Y)$ ($p > 2$) whenever (3.18) is used (see [17, Rem. 3.3]).

Macroproblem. The input parameter of the macrobilinear form $B(\cdot, \cdot)$ defined in (4.2) are given by the microsolutions u which satisfy $u - u^H \in W_{per}^1(K_\varepsilon)$ and thus

$$\int_{K_\varepsilon} (\nabla u - \nabla u^H) d\xi = 0 \quad \forall u^H \in S_0^1(\Omega, \mathcal{T}_H);$$

hence $\int_{K_\varepsilon} |\nabla u|^2 d\xi = \int_{K_\varepsilon} |\nabla u - \nabla u^H|^2 d\xi + \int_{K_\varepsilon} |\nabla u^H|^2 d\xi$, and the coercivity of $B(\cdot, \cdot)$ follows. Since

$$\int_{K_\varepsilon} \nabla u A(\xi_k, \xi/\varepsilon) (\nabla u - \nabla u^H) d\xi = 0,$$

we have $\|\nabla u\|_{L^2(K_\varepsilon)} \leq C \|\nabla u^H\|_{L^2(K_\varepsilon)}$, and the boundedness of $B(\cdot, \cdot)$ follows.

Microproblem. Let $\chi^j(\xi_k, y)$, $j = 1, 2$, be the solutions of the cell problems (3.21) in section 3.3.1. Then $\forall v \in W_{per}^1((0, 1)^2)$

$$\int_{(0,1)^2} \nabla \chi^j \frac{\partial u^H}{\partial x_j} A(\xi_k, y) (\nabla v)^T dy = - \int_{(0,1)^2} \left(e_j \frac{\partial u^H}{\partial x_j} \right) A(\xi_k, y) (\nabla v)^T dy,$$

where $\partial u^H / \partial x_j$ is constant since $u^H \in S_0^1(\Omega, \mathcal{T}_H)$. Thus, with the change of variables $y = x/\varepsilon$, we see that $u = u^H + \varepsilon \sum_{j=1}^2 \chi^j(x_k, x/\varepsilon) \frac{\partial u^H(x)}{\partial x_j}$ satisfies (3.25). A direct calculation then shows that (see [1, sect. 2.3])

$$\frac{1}{|K^\varepsilon|} \int_{K^\varepsilon} A(\xi_k, \xi/\varepsilon) \nabla u d\xi = A^0(\xi_k) \nabla u,$$

where A^0 is the homogenized matrix (see (3.20)). Finally, we obtain

$$(A.1) \quad \frac{|K|}{|K^\varepsilon|} \int_{K^\varepsilon} \nabla u A(\xi_k, \xi/\varepsilon) (\nabla v)^T d\xi = \int_K \nabla u^H A^0(\xi_k) (\nabla v^H)^T d\xi,$$

where the right-hand side will be denoted by $\tilde{B}(u^H, v^H)$.

We prove now an H^1 estimate of the difference between the solution produced by the hierarchic multiscale method defined in section 4.1 applied to problem (3.17) and the solution of the homogenized problem (3.19) which is analogous to a result of [12]. We use the bilinear form (4.2) instead of (3.24) for the problem (3.17) (the difference from [12] is that we fix the macrovariable at the barycenter on each macroelement K).

THEOREM A.1. *Let the solution u^0 of the homogenized problem (3.19) be H^2 -regular, and denote by u^H the solution of problem (3.17) with bilinear form (4.2). Then*

$$(A.2) \quad \|u^0 - u^H\|_{H^1(\Omega)} \leq CH\|f\|_{L^2(\Omega)}.$$

Proof. Let us denote by $B^0(\cdot, \cdot)$ the bilinear form of the homogenized problem (3.19). Using the first Strang lemma we have

$$(A.3) \quad \|u^H - u^0\|_{H^1(\Omega)} \leq C \inf_{v^H \in S_0^1} \left(\|u^0 - v^H\|_{H^1(\Omega)} + \sup_{w^H \in S_0^1} \frac{|B(v^H, w^H) - B^0(v^H, w^H)|}{\|w^H\|_{H^1(\Omega)}} \right),$$

where $S_0^1 = S_0^1(\Omega, \mathcal{T}_H)$ and $B(\cdot, \cdot)$ is the bilinear form defined in (4.2).

We take v_I^H to be the standard linear interpolant of u^0 . Classical results (e.g., [6]) then give $\|v_I^H - u^0\|_{H^1(\Omega)} \leq CH\|u^0\|_{H^2(\Omega)}$. It remains to estimate the second term of (A.3)

$$(A.4) \quad |B(v_I^H, w^H) - B^0(v_I^H, w^H)| \leq \sum_{K \in \mathcal{T}_H} \left| \int_K \sum_{i,j} (A_{ij}^0(\xi_k) - A_{ij}^0(\xi)) \partial_i u^H \partial_j v_I^H d\xi \right| \leq CH\|\nabla v_I^H\|_{L^2(\Omega)}\|\nabla w^H\|_{L^2(\Omega)} \leq CH\|v_I^H\|_{H^1(\Omega)}\|w^H\|_{H^1(\Omega)},$$

where we have used that $B(v_I^H, w^H) = \tilde{B}(v_I^H, w^H)$ (see (A.1)). This, together with the a priori estimate $\|u^0\|_{H^2(\Omega)} \leq C\|f\|_{L^2(\Omega)}$, gives the theorem. \square

REMARK A.2. *The estimate (A.4) can be improved (see [7]) to*

$$(A.5) \quad |B(v_I^H, w^H) - B^0(v_I^H, w^H)| \leq CH^2\|v_I^H\|_{H^1(\Omega)}\|w^H\|_{H^1(\Omega)}.$$

Using the estimate (A.5), the $H^2(\Omega)$ regularity of the homogenized solution u^0 , Theorem A.1, and the Aubin–Nitsche lemma, we get the following L^2 estimate:

$$(A.6) \quad \|u^0 - u^H\|_{L^2(\Omega)} \leq CH^2\|f\|_{L^2(\Omega)}.$$

Using estimates (A.6) and (3.18) we obtain

$$(A.7) \quad \|u^\varepsilon - u^H\|_{L^2(\Omega)} \leq C(\varepsilon + H^2)\|f\|_{L^2(\Omega)},$$

where u^ε is the solution of problem (3.17).

Further estimates are given in [11], [12],

$$(A.8) \quad \|u^\varepsilon - u_{\text{rec}}^H\|_{\bar{H}^1(\Omega)} \leq C(\sqrt{\varepsilon} + H)\|f\|_{L^2(\Omega)},$$

$$(A.9) \quad \|Pu^\varepsilon - u^H\|_{L^2(\Omega)} \leq C(\varepsilon + H^2)\|f\|_{L^2(\Omega)},$$

$$(A.10) \quad \|Pu^\varepsilon - u^H\|_{H^1(\Omega)} \leq C(\varepsilon/H + H)\|f\|_{L^2(\Omega)},$$

where P is a compression operator, for example the L^2 projection defined in (4.12), u_{rec}^H is the reconstructed solution from u^H with microscale information defined in (4.8), and \bar{H}^1 denotes the broken H^1 norm given in (4.9).

Appendix B. Lemma 2.1. *Suppose (A1) and (A2) hold. Then there exist $\varepsilon_0 > 0$ such that $\forall \varepsilon < \varepsilon_0$, $F^\varepsilon|_\Omega$ is injective.*

Proof. Suppose the contrary. Then $\forall \varepsilon_0$, there exist $\varepsilon < \varepsilon_0$ and $\xi \neq \bar{\xi}$ such that $F^\varepsilon(\xi) = F^\varepsilon(\bar{\xi})$. In particular, for the sequence $\varepsilon_0^n = 1/n$, there exist $\varepsilon^n, \xi^n \neq \bar{\xi}^n$ such that $F^{\varepsilon^n}(\xi^n) = F^{\varepsilon^n}(\bar{\xi}^n)$. There exist then subsequences of ε^n and of $\xi^n \neq \bar{\xi}^n \in \Omega$ (for which we use the same notation) such that $\varepsilon^n \rightarrow 0$, $\xi^n \rightarrow \xi$, $\bar{\xi}^n \rightarrow \bar{\xi}$ in $\bar{\Omega}$.

Suppose $\xi = \bar{\xi}$. Let κ be the maximum of the normal curvature of $\Gamma^0 = F^0(\Omega)$ at ξ . If $\kappa = 0$, (A1) implies immediately that F^ε defined by (2.1) is injective near ξ , and we obtain a contradiction. If $\kappa \neq 0$, let $r = 1/\kappa$ be the radius of the corresponding osculating sphere, and let $B_\eta(\xi)$ be the ball of radius $\eta > 0$ centered in ξ . Then by (A1) there exist $\eta > 0$ such that $\forall \xi_1 \neq \xi_2 \in B_\eta(\xi) \cap \Omega$

$$F^0(\xi_1) + \beta_1 n^0(\xi_1) = F^0(\xi_2) + \beta_2 n^0(\xi_2) \implies |\beta_1|, |\beta_2| > r/2.$$

Since $\forall n \geq N_0$ we have that $\xi^n \neq \bar{\xi}^n \in B_\eta(\xi)$, and by using (A2) we have

$$\max(|\varepsilon^n a(\xi^n/\varepsilon)n(\xi^n)|, |\varepsilon^n a(\bar{\xi}^n/\varepsilon)n(\bar{\xi}^n)|) \leq \alpha_1 \varepsilon^n \rightarrow 0,$$

and we obtain a contradiction.

Suppose $\xi \neq \bar{\xi}$, and assume $\xi, \bar{\xi} \notin \partial\Omega$. Then $|F^0(\xi^n) - F^0(\bar{\xi}^n)| > C \forall n > N_0$ since F^0 is injective by (A1). But $F^\varepsilon(\xi^n) = F^\varepsilon(\bar{\xi}^n)$ implies with (A2) that $|F^0(\xi^n) - F^0(\bar{\xi}^n)| = \varepsilon^n |a(\xi^n/\varepsilon)n^0(\xi^n) - a(\bar{\xi}^n/\varepsilon)n^0(\bar{\xi}^n)| \leq 2\varepsilon^n \alpha_1 \rightarrow 0$, which leads to a contradiction. Finally, if ξ or $\bar{\xi} \in \partial\Omega$, similar arguments lead again to a contradiction, and the proof is complete. \square

REFERENCES

- [1] A. ABDULLE AND W. E, *Finite difference HMM for homogenization problems*, J. Comput. Phys., 191 (2003), pp. 18–39.
- [2] P. M. ADLER, J.-F. THOVERT, S. BERKI, AND F. YOUSIFIAN, *Real porous media: Local geometry and transports*, J. Engineering Mechanics, 128 (2002), pp. 829–839.
- [3] I. BABUSKA, *Homogenization and its applications. Mathematical and computational problems*, in Numerical Solution of Partial Differential Equations III, B. Hubbard, ed., Academic Press, New York, 1976, pp. 89–116.
- [4] R. BAUSCH AND R. SCHMITZ, *Diffusion in the presence of topological disorder*, Phys. Rev. Lett., 73 (1994), pp. 2382–2385.
- [5] A. BENSOUSSAN, J.-L. LIONS, AND G. PAPANICOLAOU, *Asymptotic Analysis for Periodic Structures*, North-Holland, Amsterdam, 1978.
- [6] D. BRAESS, *Finite Elements*, Cambridge University Press, Cambridge, UK, 1997.
- [7] P. G. CIARLET AND P.-A. RAVIART, *The combined effect of curved boundaries and numerical integration in isoparametric finite element methods*, in The Mathematical Foundations of the Finite Element Methods with Applications to Partial Differential Equations, A. K. Aziz, ed., Academic Press, New York, 1972, pp. 409–474.
- [8] P. G. CIARLET, *The Finite Element Method for Elliptic Problems*, North-Holland, Amsterdam, 1978.
- [9] D. CIORANESCU AND P. DONATO, *An Introduction to Homogenization*, Oxford University Press, New York, 1999.
- [10] E. DIMMLER, R. MARABINI, P. TITTMANN, AND H. GROSS, *Correlation of topographic surface and volume data from three-dimensional electron microscopy*, J. Structural Biology, 136 (2001), pp. 20–29.
- [11] W. E AND B. ENGQUIST, *The heterogeneous multi-scale methods*, Commun. Math. Sci., 1 (2003), pp. 87–132.
- [12] W. E, P. MING, AND P. ZHANG, *Analysis of the Heterogeneous Multi-scale Method for Elliptic Homogenization Problems*, <http://www.math.princeton.edu/multiscale/>.
- [13] B. ENGQUIST, *Computation of oscillatory solutions to partial differential equations*, in Non-linear Hyperbolic Problems, Lecture Notes in Math. 1270, C. Carasso, P.-A. Raviart, and D. Serre, eds., Springer-Verlag, Berlin, 1987, pp. 10–22.

- [14] T. FUJIWARA, K. RITCHIE, H. MURAKOSHI, K. JACOBSON, AND A. KUSUMI, *Phospholipids undergo hop diffusion in compartmentalized cell membrane*, J. Cell Biology, 157 (2002), pp. 1071–1081.
- [15] C. GÉROT, D. ATTALI, AND A. MONTANVERT, *D'une surface triangulée à une surface représentée par cartes*, Revue Internationale de CFAO et d'Infographie: Mondes virtuels, representation et simulation, 16 (2001), pp. 9–24.
- [16] T.-Y. HOU AND X.-H. WU, *A multiscale finite element method for elliptic problems in composite materials and porous media*, J. Comput. Phys., 134 (1997), pp. 169–189.
- [17] T.-Y. HOU, X.-H. WU, AND Z. CAI, *Convergence of a multi-scale finite element method for elliptic problems with rapidly oscillating coefficients*, Math. Comp., 68 (1999), pp. 913–943.
- [18] V. V. JIKOV, S. M. KOZLOV, AND O. A. OLEINIK, *Homogenization of Differential Operators and Integral Functionals*, Springer-Verlag, Berlin, Heidelberg, 1994.
- [19] I. LUNATI, W. KINZELBACH, AND I. SORENSEN, *Effects of pore volume-transmissivity correlation on transport phenomena*, J. Cont. Hyd., 67 (2003), pp. 195–217.
- [20] A.-M. MATACHE, I. BABUSKA, AND C. SCHWAB, *Generalized p-FEM in homogenization*, Numer. Math., 86 (2000), pp. 319–375.
- [21] S. MOSKOW AND M. VOGELIUS, *First order corrections to the homogenized eigenvalues of a periodic composite medium*, Proc. Roy Soc. Edinburgh Sect. A, 127 (1997), pp. 1263–1299.
- [22] V. V. MOURZENKO, J.-F. THOVERT, AND P. M. ADLER, *Percolation and conductivity of self-affine fractures*, Phys. Rev. E (3), 59 (1999), pp. 4265–4284.
- [23] J. T. ODEN AND K. S. VEMAGANTI, *Estimation of local modeling error and global-oriented adaptive modeling of heterogeneous materials: Error estimates and adaptive algorithms*, J. Comput. Phys., 164 (2000), pp. 22–47.
- [24] C. SCHWAB AND A.-M. MATACHE, *Generalized FEM for homogenization problems*, in Multiscale and Multiresolution Methods, Lect. Notes Comput. Sci. Eng. 20, T. J. Barth, T. F. Chan, and R. Haimes, eds., Springer-Verlag, Berlin, 2002, pp. 197–238.